Tools for Modeling Beam Dynamics in Rings Based on Nonlinear Integrable Optics

Chad Mitchell, Lawrence Berkeley National Laboratory

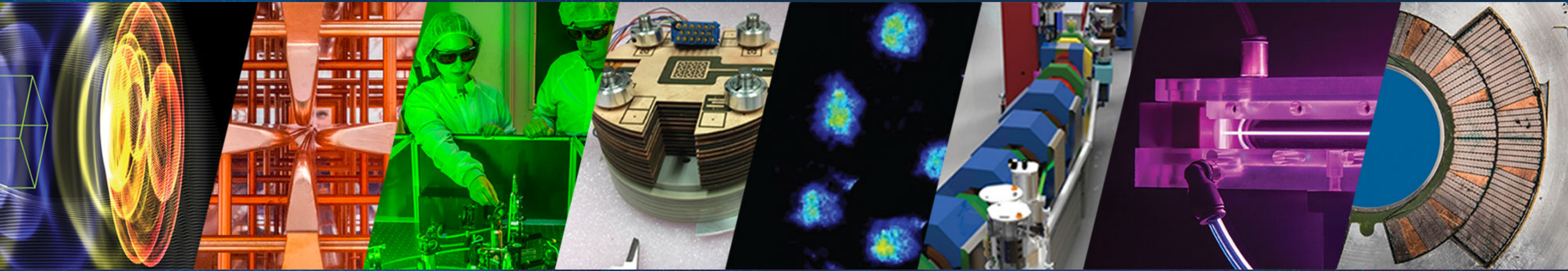

14th International Computational Accelerator Physics Conference

October 2-5, 2024

BERKELEY LAB

ACCELERATOR TECHNOLOGY & APPLIED PHYSICS DIVISION ATAP

U.S. DEPARTMENT OF ENERGY | Office of Science

Advanced Modeling Program

Acknowledgements

Thanks to the organizing committee and to collaborators, including especially:

- Kilean Hwang (MSU) and Rob Ryne (LBNL affiliate)
- Sasha Valishev, Sasha Romanov, Jeff Eldred (FNAL)
- David Bruhwiler, Chris Hall, Nathan Cook (RadiaSoft)
- Finn O’Shea (formerly RadiaBeam)
- Yongjun Li, Sergei Nagaitsev (Brookhaven)

This work was supported by the DOE Office of Science, Office of High Energy Physics, and made use of computing resources at the National Energy Research Scientific Computing Center.

Outline

- *Nonlinear integrable beam optics in rings*

- *Computational and theoretical tools*
  - *single-particle dynamics – tracking, analytical methods*
  - *collective effects – space charge, matching, relaxation*
  - *numerical diagnostics – chaos, filamentation, losses*

- *Optimization for halo suppression*

- *Conclusions*

- **Nonlinear Integrable Beam Optics in Rings**

The IOTA storage ring : an accelerator R&D test facility with a focus on strategies to mitigate space charge-induced beam halo.

- **Possible solutions: electron lenses and columns, nonlinear integrable lattices**

- **Integrable Optics Test Accelerator (IOTA)**

  - Novel accelerator physics: strongly nonlinear design
  - Experimental test bed for space charge mitigation
  - Run first with electrons, then low-energy protons

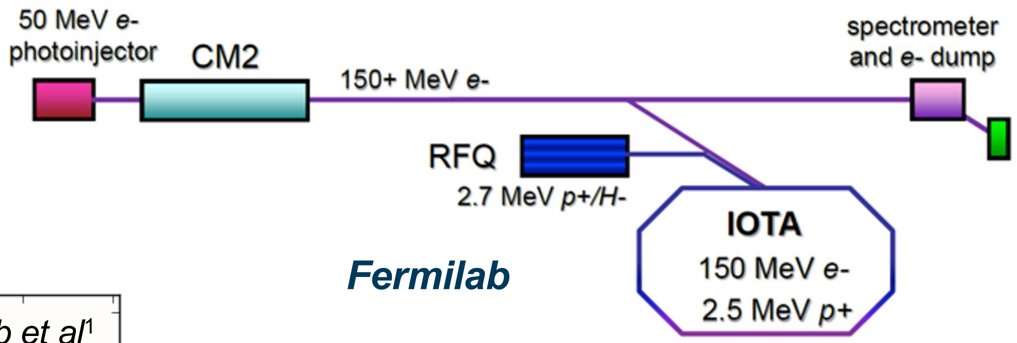

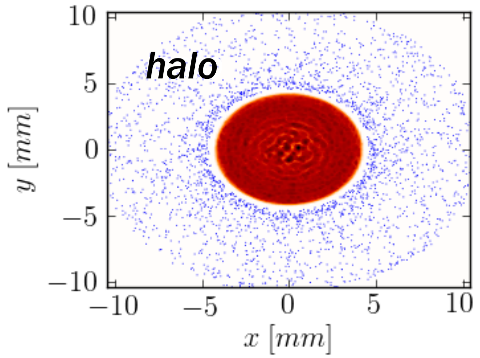

using conventional linear design

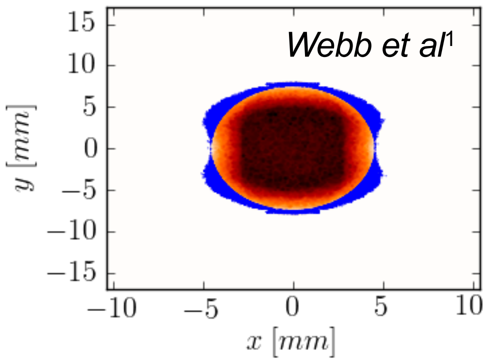

using nonlinear integrable design

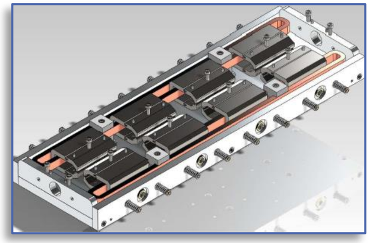

nonlinear magnetic insert

- **Nonlinearity ➡ tune spread "washes out" instabilities, core-halo resonances**
- **Integrability ➡ ensures orbits are regular and remain bounded (no chaos)**

S. Danilov, S. Nagaitsev, PRAB 13, 084002 (2010)
S. Antipov *et al*, JINST **12**, T03002 (2017)
[1]S. Webb et al, p. 2961, IPAC 2012

Integrability = the single-particle orbits are confined to level sets defined by invariants of motion ➡ motion with stable frequencies (tunes)

Liouville-Arnold Theorem

Suppose H is a time-independent Hamiltonian for an n degree-of-freedom system, and $H = f_1, f_2, \ldots, f_n$ are n smooth functions on the phase space M such that:

invariants

1) $\nabla f_1, \ldots, \nabla f_n$ are linearly independent (the f_j are *independent*)

2) $\{f_i, f_j\} = 0 \quad (i, j = 1, \ldots, n)$ (the f_j are *in involution*)

level sets

$\Longrightarrow$ The motion is confined to a set $M_z = \{p \in M | f_i(p) = z_i, i = 1, \ldots, n\}$.

If M_z is compact and connected, then M_z is diffeomorphic to the n-torus.

original variables

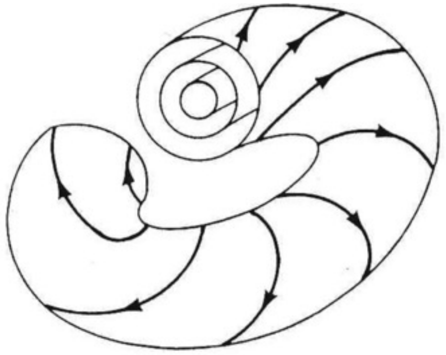

smooth coordinate transformation

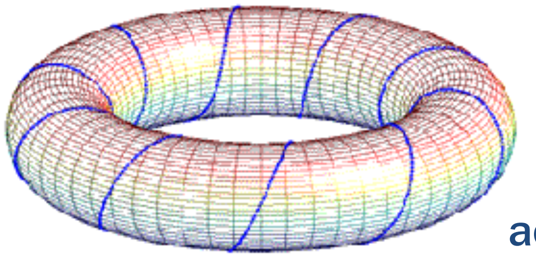

action-angle variables

Examples:
- stable linear motion
- nonlinear pendulum
- 2-body Keplerian motion

Similar definitions apply to symplectic maps.

Fermilab's IOTA Ring: Nonlinear Integrable Optics Lattice Configuration

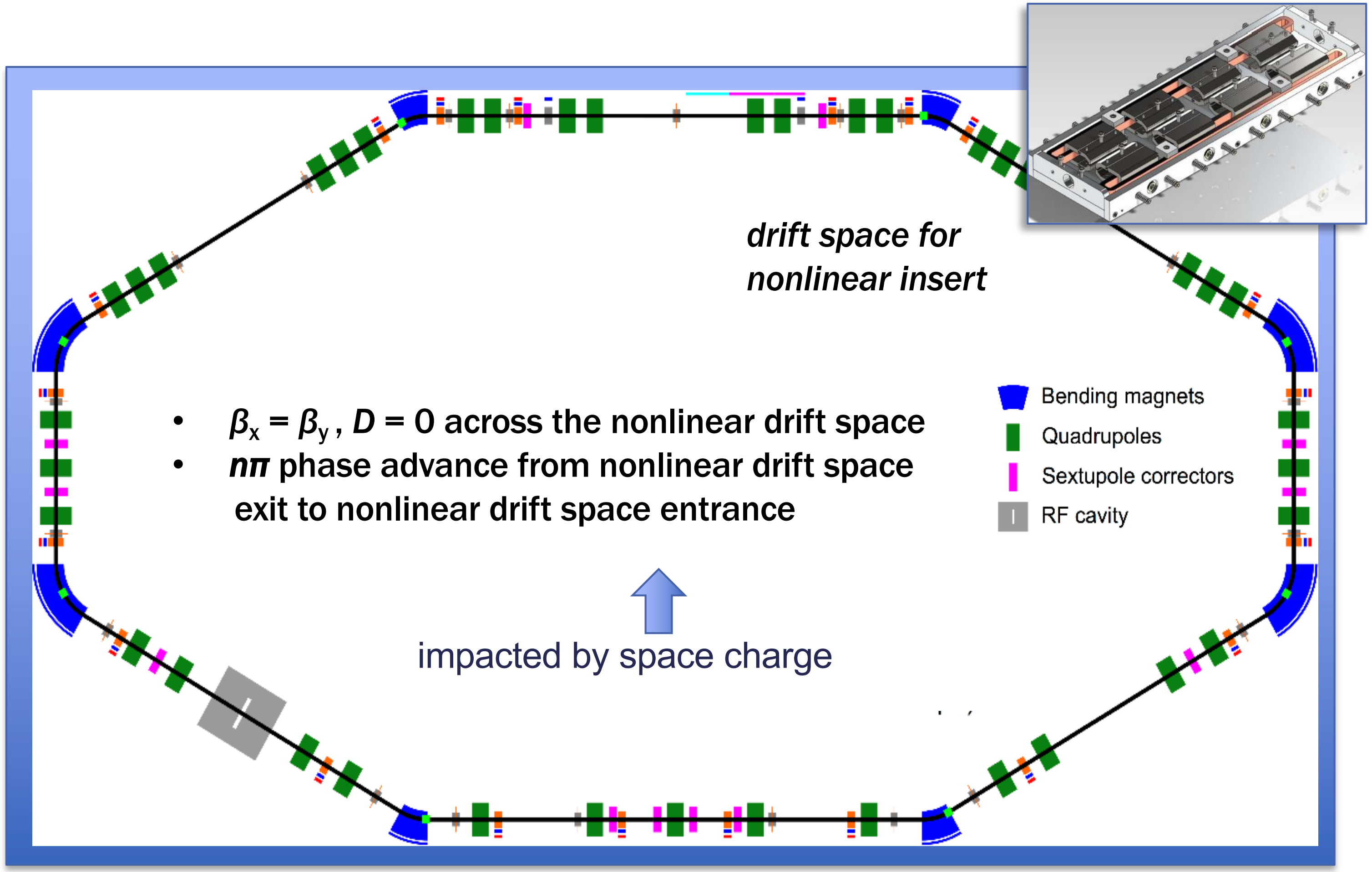

- $\beta_x = \beta_y$, $D = 0$ across the nonlinear drift space
- $n\pi$ phase advance from nonlinear drift space exit to nonlinear drift space entrance

Two invariants of the transverse motion.*
H - single-particle Hamiltonian
I – second invariant

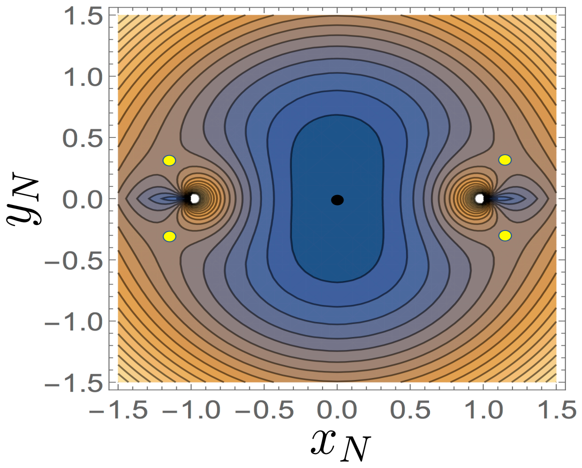

Equivalent to integrable motion in a 2D nonlinear potential

IOTA's experimental program also includes:
- *use of electron lenses and columns*
- *optical stochastic cooling*
- *single-electron quantum science*

*S. Danilov and S. Nagaitsev, PRAB **13**, 084002 (2010).
S. Antipov *et al*, JINST **12**, T03002 (2017)

R&D Areas: Long-Time Beam Prediction at the Interface Between Nonlinear Dynamics and High Intensity

Advanced Algorithm Development *(Goals: improved speed and fidelity of modeling on long time scales.)*

- **Fast symplectic tracking** in nonlinear applied fields/fringe fields (non-split Hamiltonians)
- Improved **integration** of realistic **3D Maxwellian RF and magnet** models with tracking tools
- **Structure-preserving space charge** modeling to ensure phase space preservation
- Improved integration of **space charge with s-based tracking** (e.g., long, bunched beams, dipoles)
- Efficient **space charge** modeling **at high resolution** (adaptive mesh refinement, higher-order particle shapes)
- Addressing **computational bottlenecks** (eg., fast in-situ numerical phase space diagnostics to reduce I/O)

Mathematical and Theoretical Methods *(Goals: validation and physics understanding for effective design.)*

- **Nonlinear methods** (e.g. Lie methods, near-integrable dynamical systems) – dynamic aperture
- Self-consistent **beam equilibria and stability** with nonlinear focusing – matching
- Understanding **numerical artifacts (particle noise)** associated with long-term simulation
- Theoretical models of space-charge-induced **beam halo formation** with nonlinear focusing
- Theoretical models of **collective instabilities** and nonlinear **decoherence** (Landau damping)

IMPACT: Multi-Physics High-Intensity and High Brightness Beam Dynamics Code Suite

- **Key features include:**
  - *time-dependent and position dependent PICs*
  - *serial and massive parallelization*
  - *detailed 3D RF accelerating and focusing model*
  - *standard elements: dipole, solenoid, multipole, etc.*
  - *multiple charge states, multiple bunches*
  - *3D space charge effects*
  - *structure and resistive wall wakefields*
  - *coherent synchrotron radiation (CSR)*
  - *incoherent synchrotron radiation (ISR)*
  - *photo-electron emission*
  - *machine errors and steering*
- **The IMPACT code suite is used by > 40 institutes worldwide**
  - *successfully applied to both electron & proton machines:*
    - ***CERN PS2 ring, SNS linac, …***
    - *LCLS-II linac*
  - *microbunching simulated using 2B macroparticles*

Start-to-end simulation of the Linac Coherent Light Source

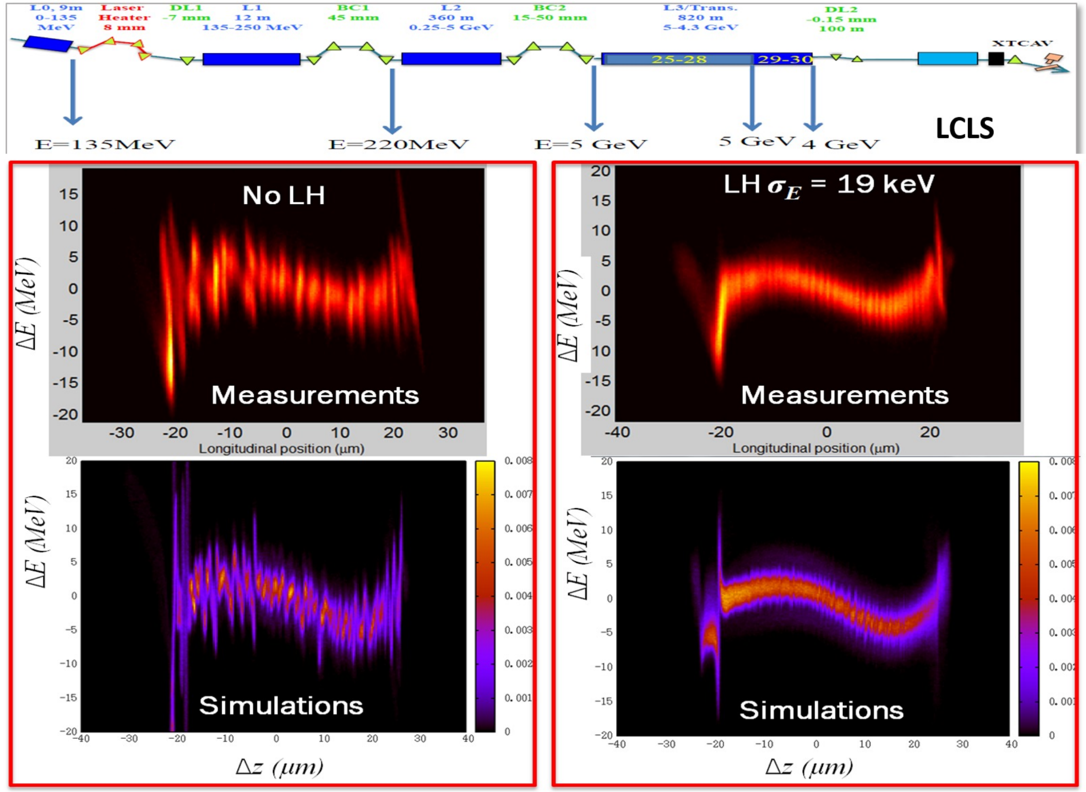

J. Qiang et al., Phys. Rev. Accel. Beams 20, 054402 (2017).

https://blast.lbl.gov/

BLAST BEAM PLASMA & ACCELERATOR SIMULATION TOOLKIT

- Single-particle dynamics

New algorithms and numerical capabilities added to IMPACT-Z to address challenges of modeling nonlinear integrable dynamics.

Implementation of the nonlinear magnetic insert using a symplectic integrator

Field lines of the nonlinear insert in the transverse plane

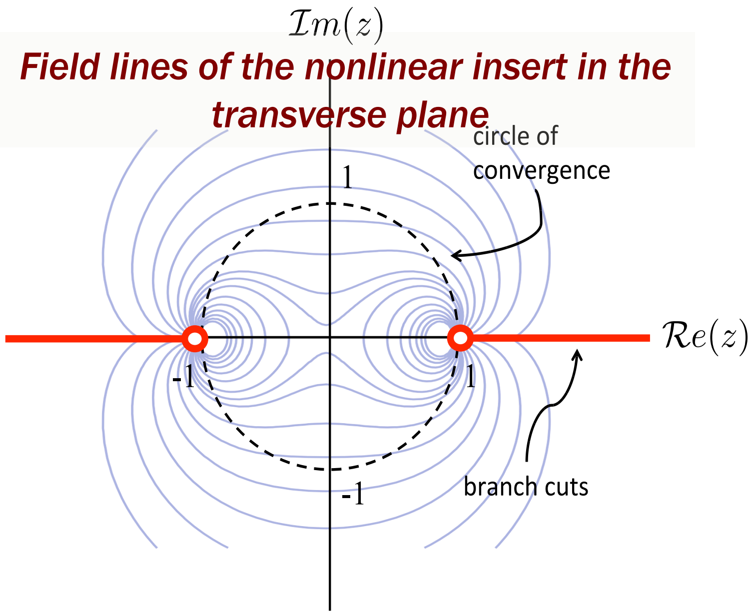

- Concise, complex representation of the nonlinear integrable potential.
- Uses a 2nd order symplectic integrator to perform *s*-dependent tracking.
- Avoids instability of previous integrators due to vanishing denominators in equations of motion.
- Additional tools for soft-edge fringe fields.

Longitudinal variation of quadrupole gradient

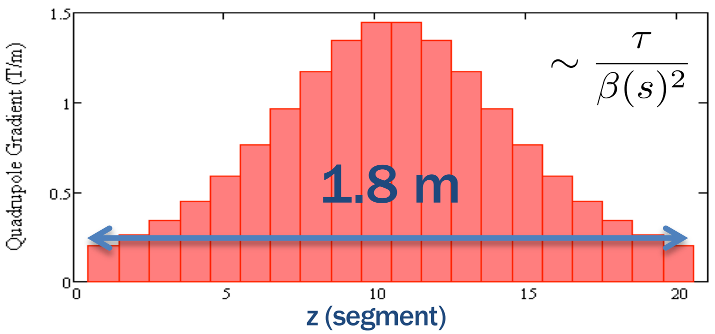

The map for a single numerical step of size *h*:

$$\mathcal{M}(s \to s+h) = \mathcal{M}_{drift}\left(\frac{h}{2}\right)\mathcal{M}_{NLL}\left(h, s+\frac{h}{2}\right)\mathcal{M}_{drift}\left(\frac{h}{2}\right) + O(h^3)$$

New algorithms and numerical capabilities added to IMPACT-Z to address challenges of modeling nonlinear integrable dynamics.

Implementation of the nonlinear magnetic insert using a symplectic integrator

Field lines of the nonlinear insert in the transverse plane

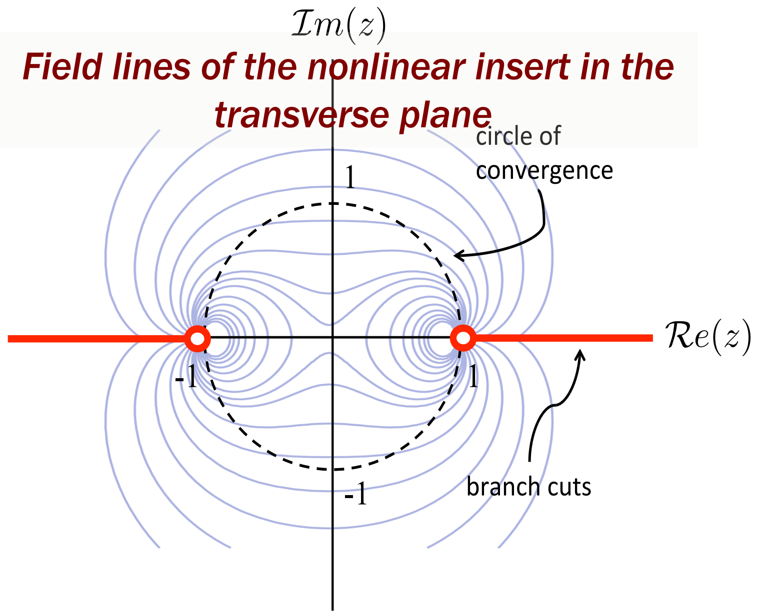

- Concise, complex representation of the nonlinear integrable potential.
- Uses a 2nd order symplectic integrator to perform *s*-dependent tracking.
- Avoids instability of previous integrators due to vanishing denominators in equations of motion.
- Additional tools for soft-edge fringe fields.

Longitudinal variation of quadrupole gradient

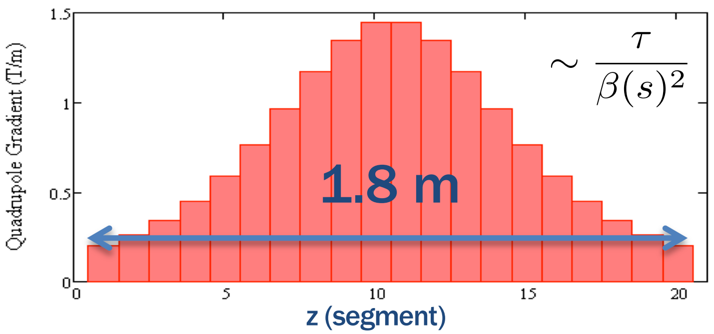

Nonlinear quadrupole fringe field effects

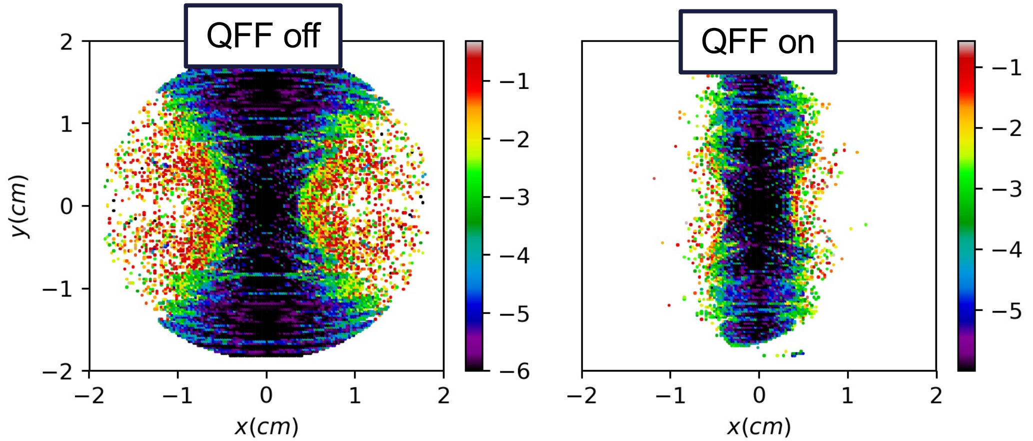

Other new capabilities implemented in IMPACT-Z

- *Python interface* and postprocessing control using *Jupyter*.
- Implementation of *quadrupole and dipole* nonlinear *fringe field* models relevant for modeling proton rings at low-moderate energy.
- Additional *Poisson solvers* and *diagnostics* capabilities (discussed later).

C. Mitchell, in *Proceedings NOCE 2017*, and *IPAC 2018*, and arXiv:1908.00036

Geometric methods in nonlinear dynamics provide a foundation for the analysis of single-particle optics in integrable accelerator lattices.

- **Need:** To understand the global single-particle dynamics accessible in accelerator designs (such as IOTA) based on nonlinear integrable optics.
- **Problem:** Standard approaches to nonlinear dynamics in the accelerator community are perturbative, neglect fully 4D or 6D coupling, or require a clever choice of coordinates.
- **Solution:** **Geometric methods** from the theory of integrable Hamiltonian systems may be applied to locate **fixed points**, periodic orbits, **dynamical bifurcations**, and determine **frequencies of motion (tunes)**, using knowledge only of **the invariants of motion.**

Reveals new operating points for the IOTA ring and guidance for future accelerator designs.

Critical initial conditions at nominal IOTA insert strength

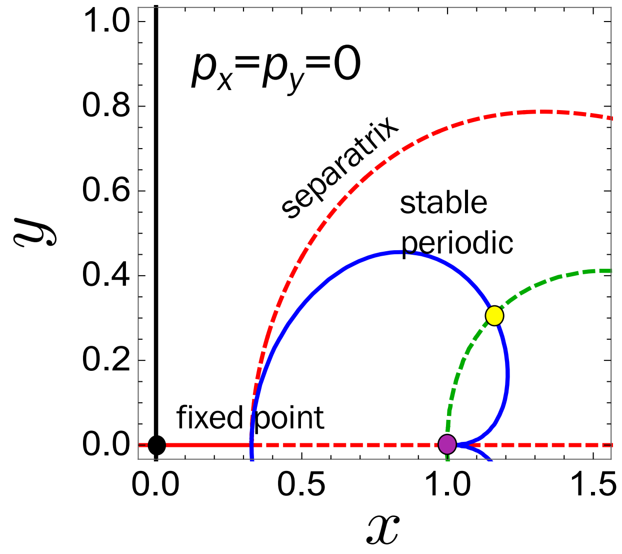

Bifurcations of dynamical fixed points in IOTA vs. magnetic insert strength

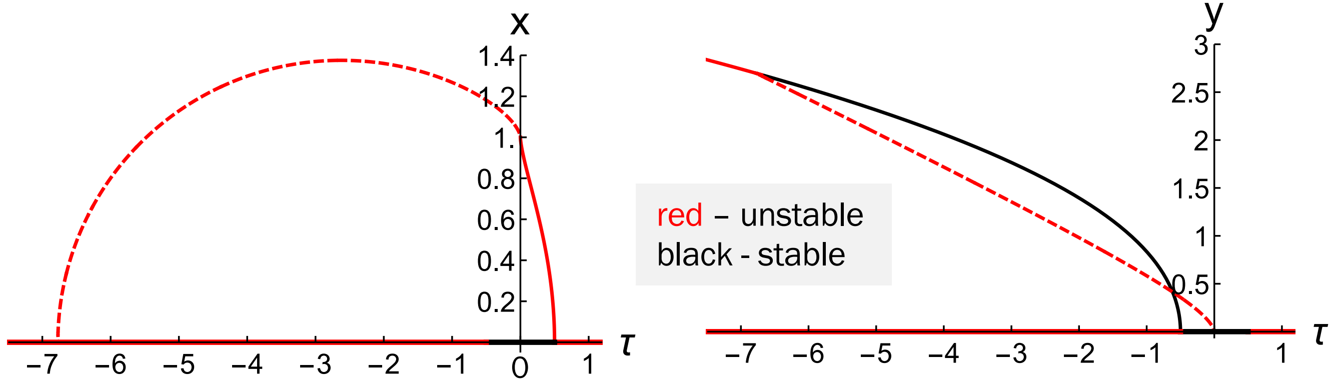

C. Mitchell et al, Phys. Rev. E 103, 062216 (2021)

C. Mitchell, K. Hwang, R. Ryne, Phys. Rev. Accel. Beams 23, 064002 (2020)

Structure of invariant level sets near the separatrix

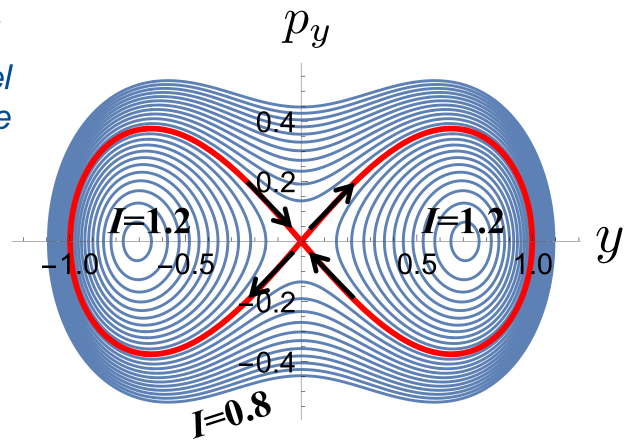

Geometric methods in nonlinear dynamics provide a foundation for the analysis of single-particle optics in integrable accelerator lattices.

- **Need:** To understand the global single-particle dynamics accessible in accelerator designs (such as IOTA) based on nonlinear integrable optics.
- **Problem:** Standard approaches to nonlinear dynamics in the accelerator community are perturbative, neglect fully 4D or 6D coupling, or require a clever choice of coordinates.
- **Solution:** **Geometric methods** from the theory of integrable Hamiltonian systems may be applied to locate **fixed points**, periodic orbits, **dynamical bifurcations**, and determine **frequencies of motion (tunes)**, using knowledge only of **the invariants of motion.**

Reveals new operating points for the IOTA ring and guidance for future accelerator designs.

Critical initial conditions at nominal IOTA insert strength

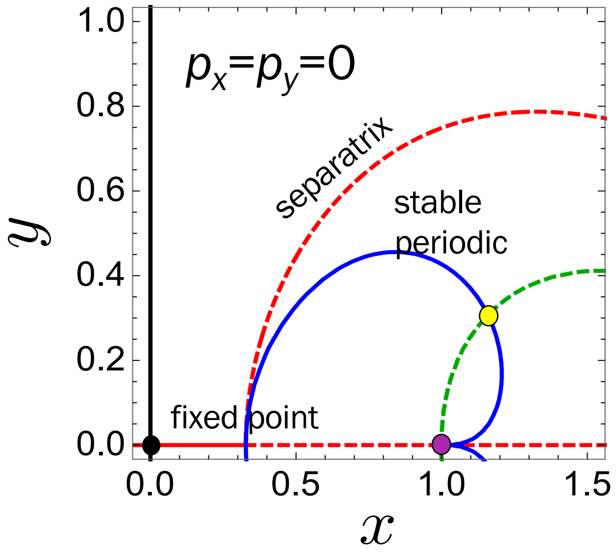

Bifurcations of dynamical fixed points in IOTA vs. magnetic insert strength

τ=-1/2 bifurcation observed during IOTA experimental run

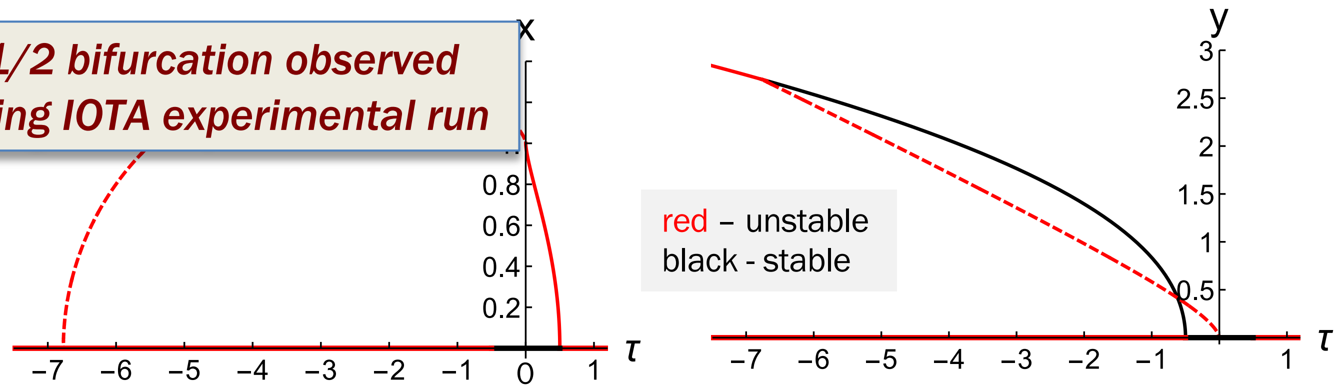

C. Mitchell et al, Phys. Rev. E 103, 062216 (2021)

C. Mitchell, K. Hwang, R. Ryne, Phys. Rev. Accel. Beams 23, 064002 (2020)

Structure of invariant level sets near the separatrix

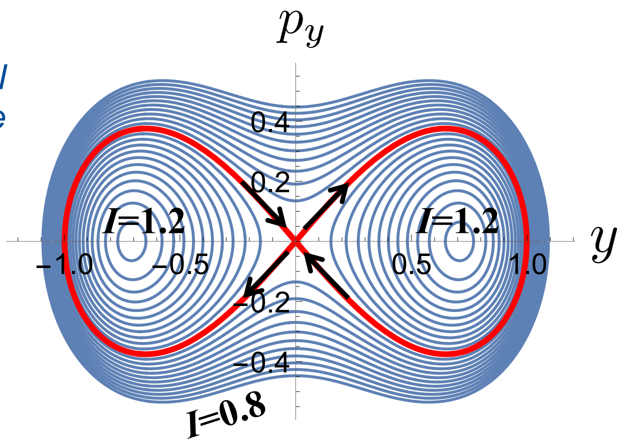

Example: Bifurcation diagram for nominal single-particle dynamics in IOTA

Bifurcation diagram showing critical values of (H,I)

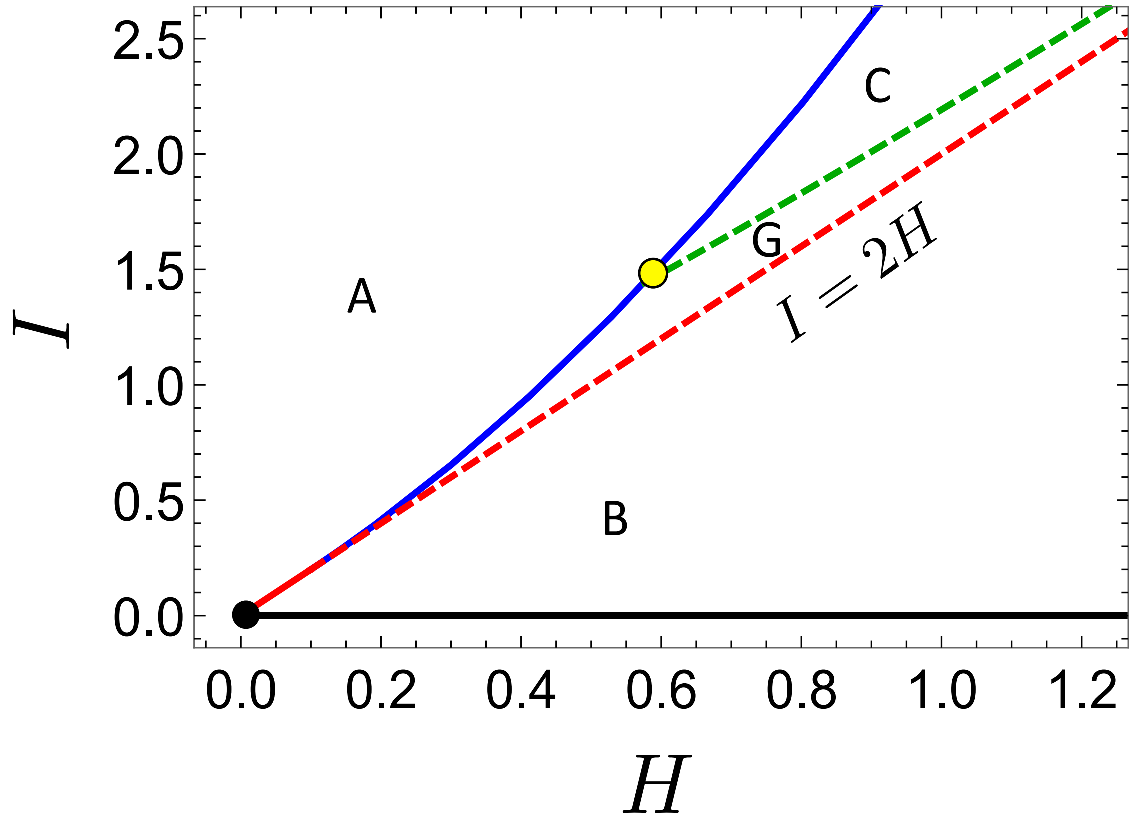

Distinct regions of the diagram correspond to dynamics with qualitatively distinct single-particle orbits.

Invariants of single-particle motion

$$H = \frac{1}{2}(p_x^2 + p_y^2 + x^2 + y^2) - \tau U(x + iy)$$

$$U(z) = \mathcal{R}e\left(\frac{z}{\sqrt{1 - z^2}}\arcsin(z)\right)$$

$$I = (xp_y - yp_x)^2 + p_x^2 + x^2 - \tau W(x + iy)$$

$$W(z) = \mathcal{R}e\left(\frac{z + \bar{z}}{\sqrt{1 - z^2}}\arcsin(z)\right)$$

Critical points occur where: $dH \wedge dI = 0$

Curves parameterizing the critical values can be determined exactly using symbolic methods *eg*, *Mathematica*.

BERKELEY LAB
ACCELERATOR TECHNOLOGY & APPLIED PHYSICS DIVISION ATAP
U.S. DEPARTMENT OF ENERGY | Office of Science

Example: Bifurcation diagram for nominal single-particle dynamics in IOTA

Bifurcation diagram showing critical values of (H,I)

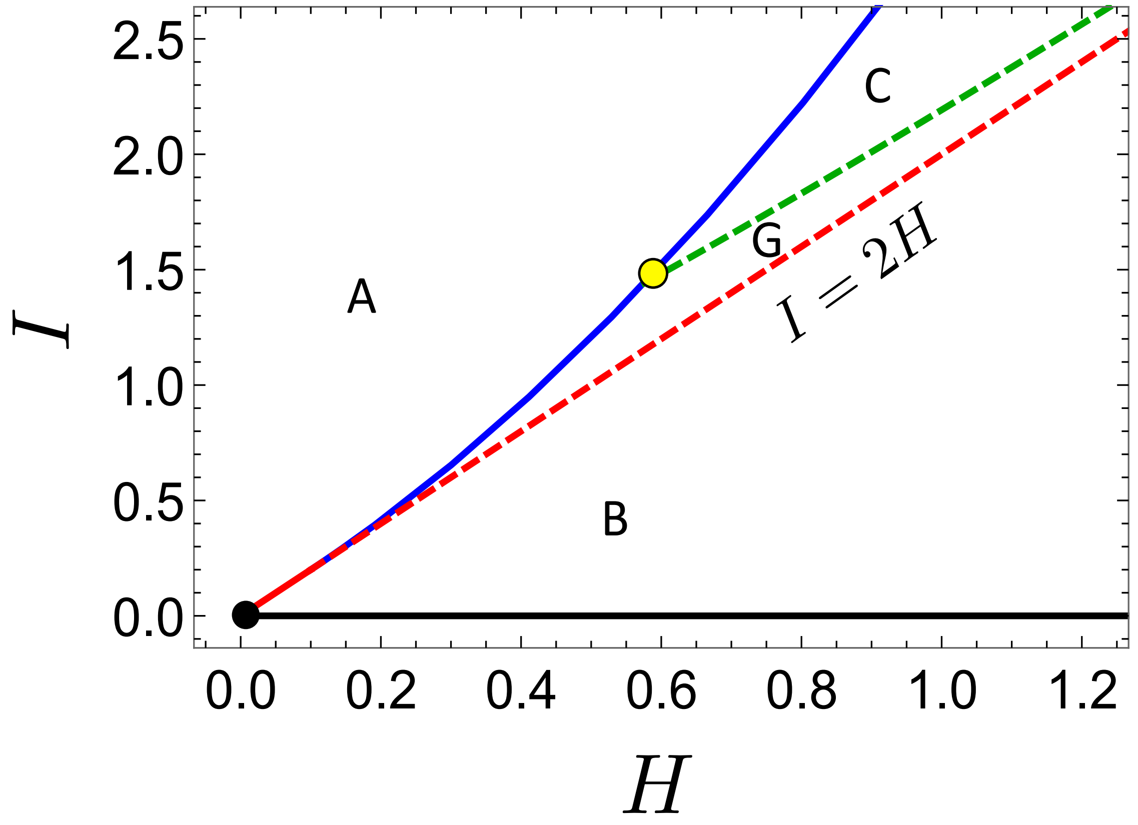

Distinct regions of the diagram correspond to dynamics with qualitatively distinct single-particle orbits.

Examples: level sets (projected onto the x-y plane)

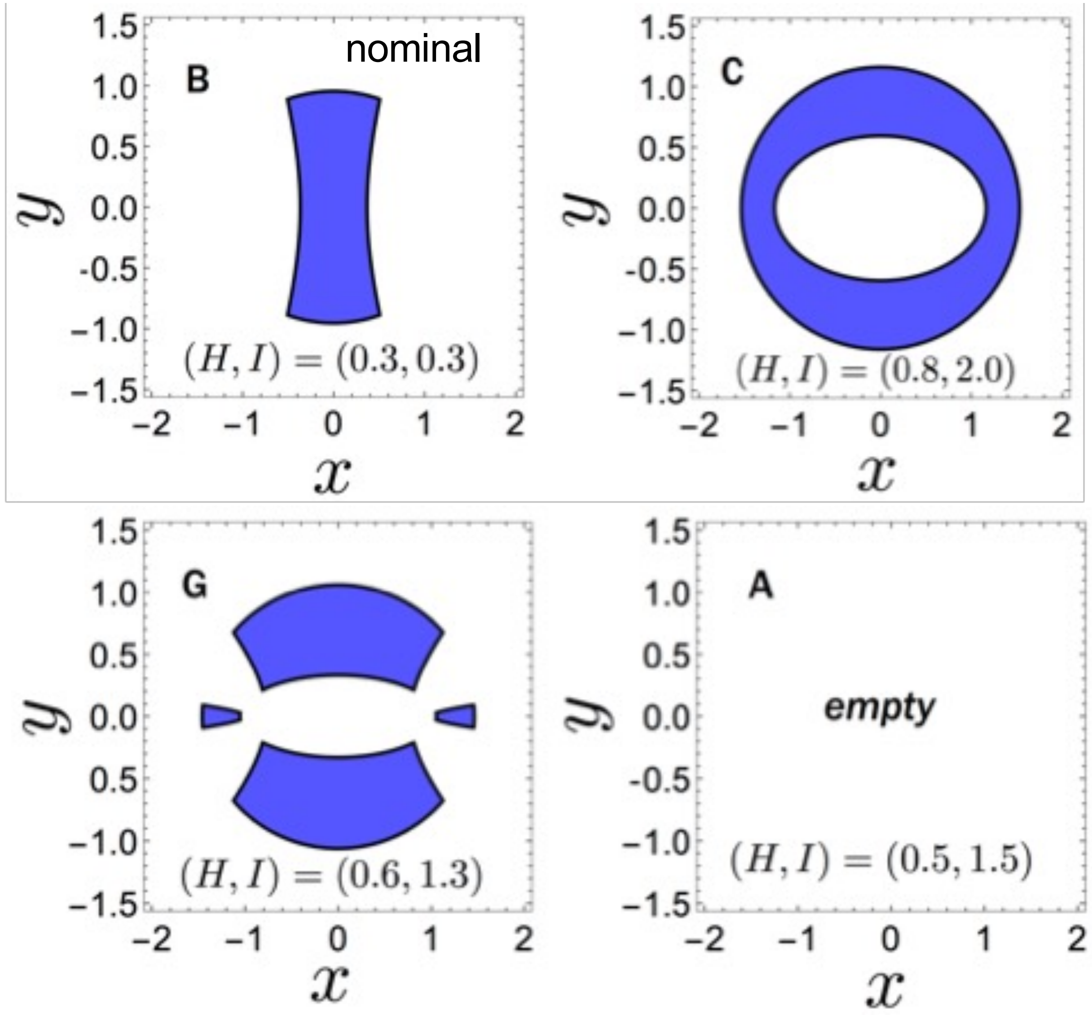

Analytical method for extracting nonlinear tunes of integrable symplectic maps developed and applied to the IOTA ring

- **Need:** To understand *analytically* the frequency content of orbits in accelerator lattices based on nonlinear integrable optics, and to use this information in accelerator design (to control tune spread).

- **Problem:** Traditional method for analysis of integrable systems relies on action-angle coordinates, which are difficult to obtain in explicit form, and which break down near critical phase space structures (*eg*, separatrices).

- **Solution:** A **semi-analytical** method to extract dynamical **tunes** of an integrable symplectic map from its **invariants of motion**, without the need for tracking, using path integrals in the invariant level sets.

Reveals the link between frequencies and geometry of level sets.
Can aid in design of future nonlinear integrable lattices.

vector of tunes

$$\nu = R^{-1} S$$

$$S = -\int_\gamma \left(D\mathcal{F}^+\right)^T J d\zeta,$$

$$R_{jk} = \left(-\oint_{\gamma_k} \left(D\mathcal{F}^+\right)^T J d\zeta\right)_j$$

C. Mitchell et al, Phys. Rev. E 103, 062216 (2021)

Extracting frequencies of the 4D McMillan mapping from its 2 invariants of motion

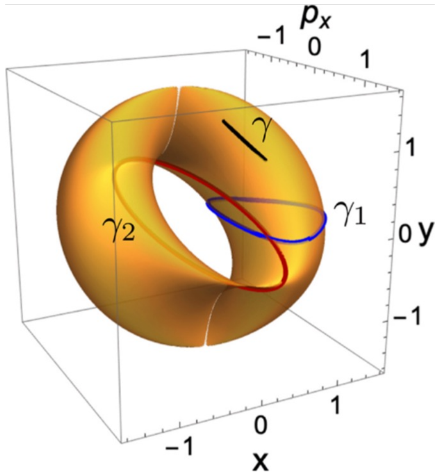

Extracting tunes for orbits in IOTA for comparison with tracking using NAFF

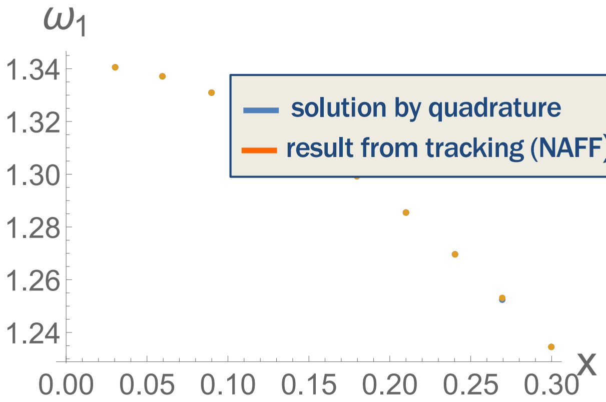

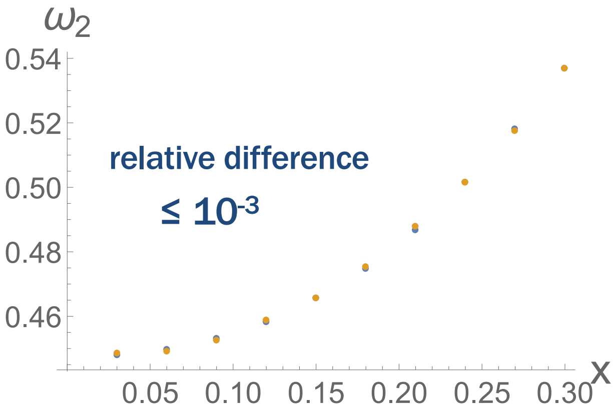

- Collective effects

Implementation of a gridless symplectic space charge solver to enable long-term Hamiltonian tracking of high intensity beams

- **Need:** Avoid numerical artifacts due to space charge that break the geometric Hamiltonian structure, necessary to ensure reliability on long time scales.

- **Problem:** Most PIC methods result in a particle push that is not symplectic on the phase space due, e.g. due to interpolation and finite differencing.

- **Solution:** A **2D gridless symplectic** space charge solver (J. Qiang, 2017) was implemented in IMPACT-Z to enable robust long-term tracking with space charge. Each step is a map that is symplectic on the collective N-body phase space of the simulated particles.

Avoids the destruction of integrability due to non-symplectic artifacts.

Evolution of the N-particle Hamiltonian

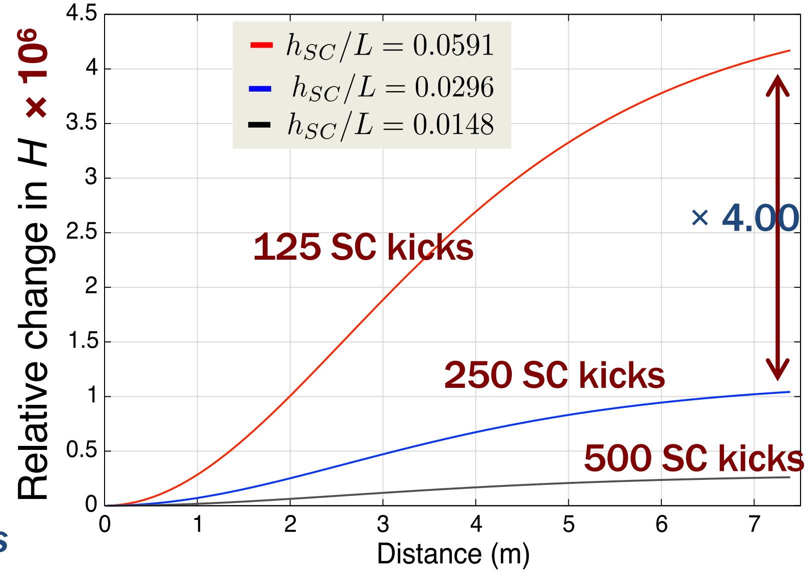

Evolution of H for a cylindrical proton beam expanding to twice its initial radius

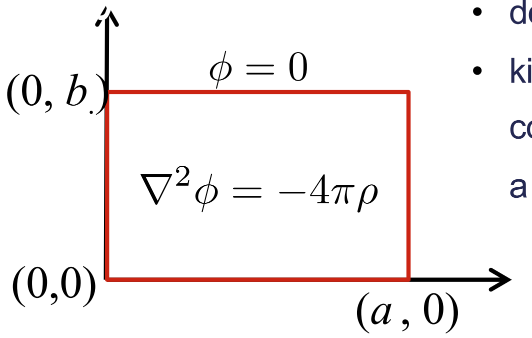

- decomposition into 2D Fourier modes
- kick is a function of the N_p particle coordinates, derived from a Hamiltonian H

$$H = \sum_{i=1}^{N_p} \frac{\mathbf{p}_i^2}{2} + 4\pi \frac{K}{2}\frac{4}{ab}\frac{1}{N_p}\sum_{i=1}^{N_p}\sum_{j=1}^{N_p}\sum_{l=1}^{N_l}\sum_{m=1}^{N_m}\frac{1}{\gamma_{lm}^2}\sin(\alpha_l x_j)\sin(\beta_m y_j)\sin(\alpha_l x_i)\sin(\beta_m y_i)$$

Computational complexity

$$O(N_l \times N_m \times N_p)$$

J. Qiang, Phys. Rev. ST Accel. Beams 20, 014203 (2017)

New PDE solver enables the study of intense beam equilibria in strongly nonlinear lattices and relaxation to equilibrium

- **Need:** To understand 4D beam Vlasov equilibria for intense beams in constant focusing channels with strongly nonlinear transverse focusing.
- **Problem:** Existing theories of beam equilibria were developed assuming linear external focusing. Few analytical models in the nonlinear case.
- **Solution:** A **spectral Galerkin solver** was developed to solve a **nonlinear PDE** for the equilibrium space charge potential. The new solver was applied to study **intense beam equilibria** in a nonlinear constant-focusing **model of IOTA**.

Reveals the expected structure of high intensity stable beams in IOTA.

Equilibrium beam, IOTA nonlinear channel, 60 mA

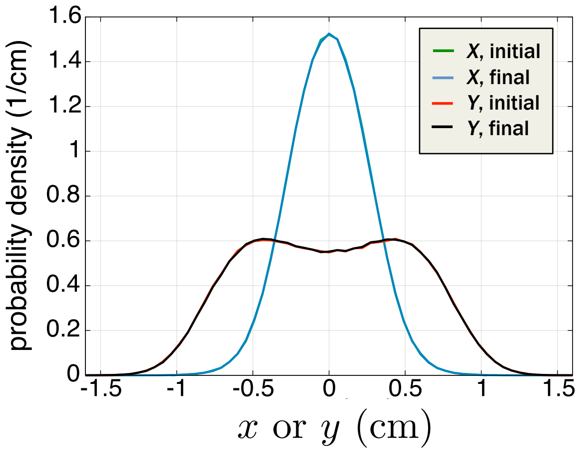

Non-equilibrium beam, IOTA nonlinear channel, 60 mA

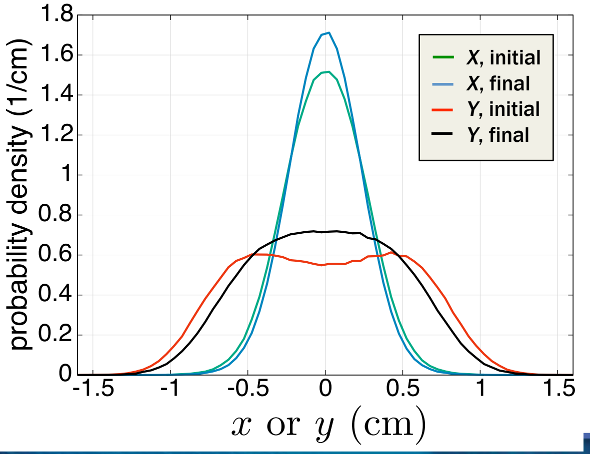

Zero current

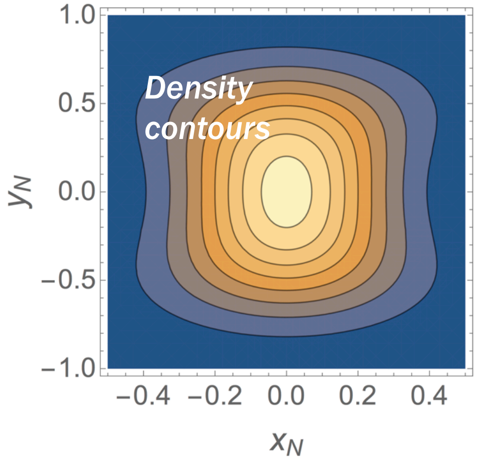

60 mA current

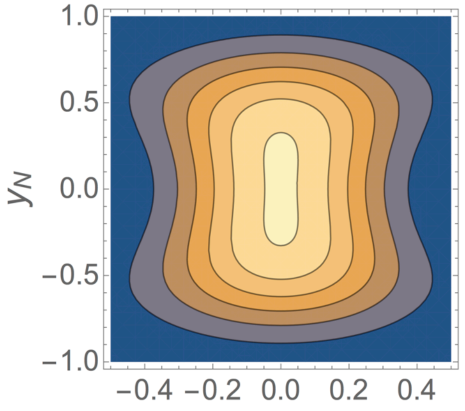

120 mA current

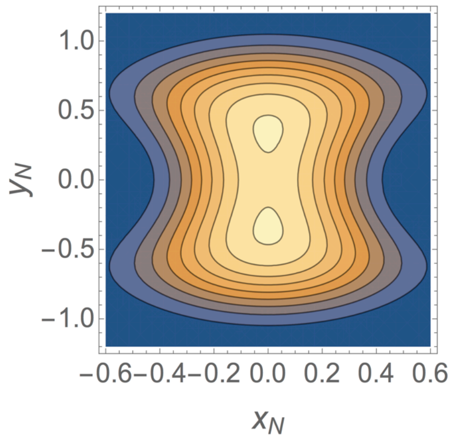

Contours illustrating equilibrium beam density in the x-y plane for increasing value of beam current

C. Mitchell, R. Ryne, K. Hwang Phys. Rev. E 100, 053308 (2020)

C. Mitchell, K. Hwang, R. Ryne J. Instrum. 15, P07019 (2020)

New PDE solver enables the study of intense beam equilibria in strongly nonlinear lattices and relaxation to equilibrium

- **Need:** To understand 4D beam Vlasov equilibria for intense beams in constant focusing channels with strongly nonlinear transverse focusing.
- **Problem:** Existing theories of beam equilibria were developed assuming linear external focusing. Few analytical models in the nonlinear case.
- **Solution:** A **spectral Galerkin solver** was developed to solve a **nonlinear PDE** for the equilibrium space charge potential. The new solver was applied to study **intense beam equilibria** in a nonlinear constant-focusing **model of IOTA**.

Reveals the expected structure of high intensity stable beams in IOTA.

Equilibrium beam, IOTA nonlinear channel, 60 mA

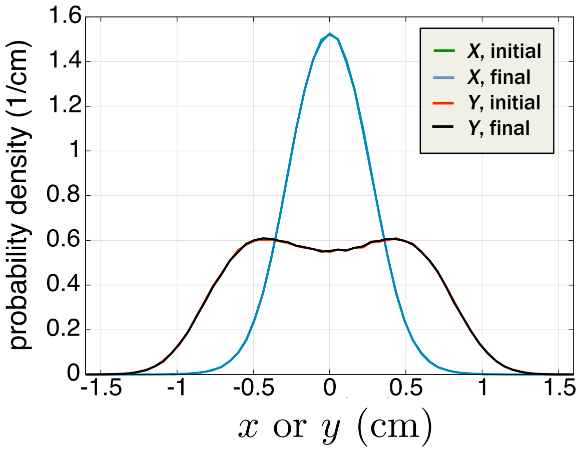

Non-equilibrium beam, IOTA nonlinear channel, 60 mA

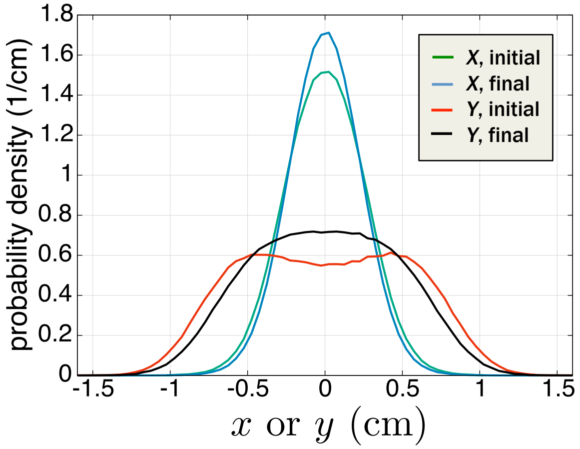

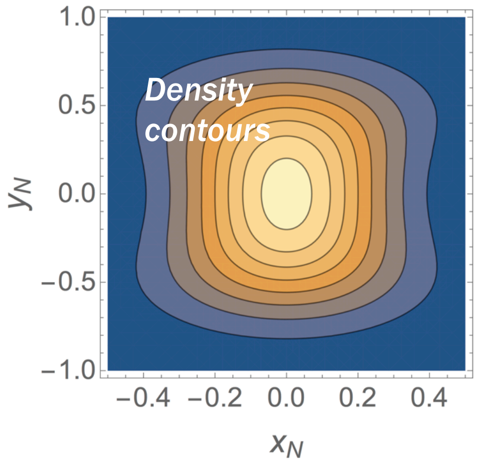

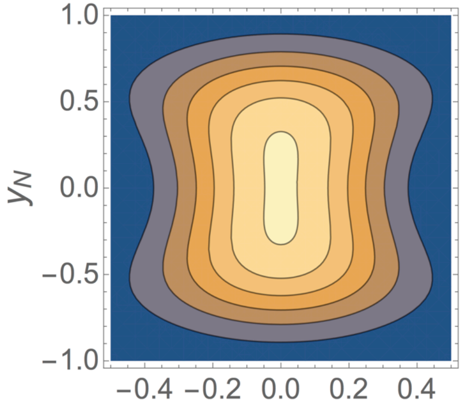

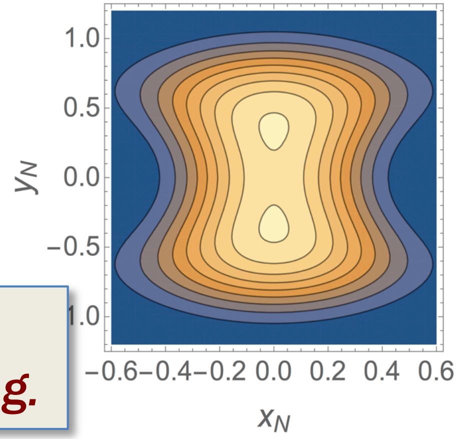

Contours illustrating equilibrium beam density in the x-y plane for increasing value of beam current

Guidance for matching injected beams using phase space painting.

C. Mitchell, R. Ryne, K. Hwang Phys. Rev. E 100, 053308 (2020)

C. Mitchell, K. Hwang, R. Ryne J. Instrum. 15, P07019 (2020)

General procedure for the generation of an initial beam distribution matched to the periodic nonlinear lattice

Beam is matched to the nonlinear lattice at the NLI midpoint.

normalized phase space variables (x_N , p_{xN} , y_N , p_{yN})

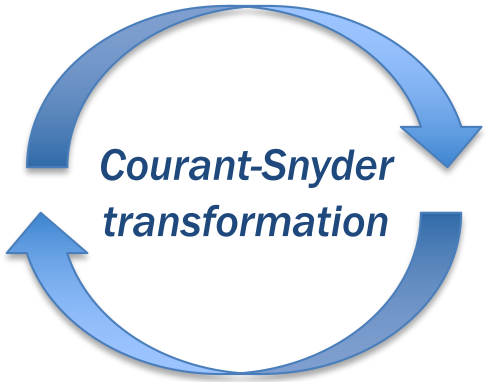

physical phase space variables (x, p_x, y, p_y)

"nonlinear KV distribution" [1]

$$f \sim \delta(H - \epsilon_0)$$

"nonlinear waterbag distribution"

$$f \sim \Theta(\epsilon_0 - H)$$

- Hamiltonian is *s*-independent
- distribution function is stationary

- Hamiltonian is *s*-dependent
- distribution varies periodically in *s*
- parameter ε_0 plays the role of emittance

$$\begin{pmatrix} x_N \\ p_{xN} \end{pmatrix} = \begin{pmatrix} 1/\sqrt{\beta} & 0 \\ \alpha/\sqrt{\beta} & \sqrt{\beta} \end{pmatrix} \begin{pmatrix} x \\ p_x \end{pmatrix}$$

boundary = equipotential curve of the nonlinear potential

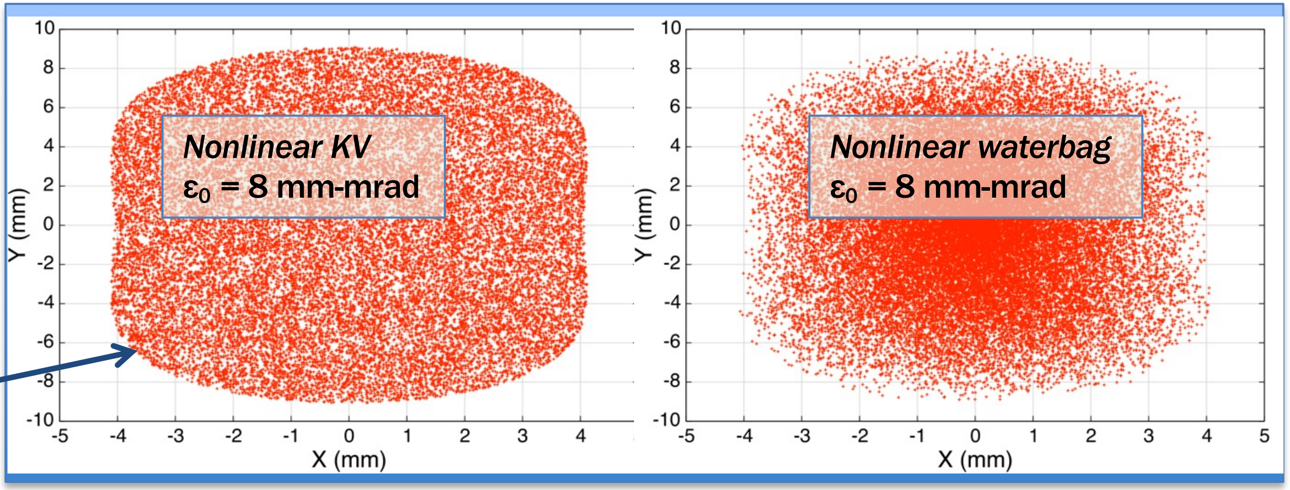

With space charge, adiabatic ramping of beam current

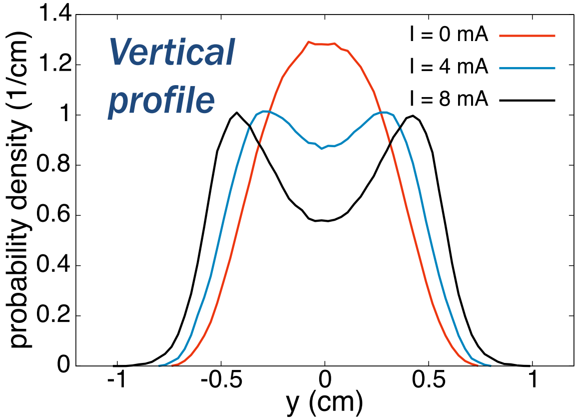

Ramping 0-8 mA over 100 turns.

Distribution at nominal 8 mA current is visibly well-matched.

High-intensity matched beam exhibits features similar to the equilibrium in a CF channel.

[1] S. Webb *et al*, p. 3099, IPAC 2013.

- **Numerical diagnostics**

Efficient numerical algorithms reveal the boundary between chaos and integrability in nonlinear integrable lattices with space charge

- **Need:** Accurate tools to distinguish between regular and chaotic motion that do not require long computing times.
- **Problem:** Standard chaos indicators (NAFF) require long time series, and space charge introduces spurious frequency drift and numerical noise.
- **Solution:** Use **symplectic** and **time-reversible** tracking algorithms and an efficient **chaos indicator using forward-backward integration**. Self-consistent tracking and idealized models of space charge **reveal similar structure**.

Nonlinear resonance lines in IOTA model with space charge tune shift

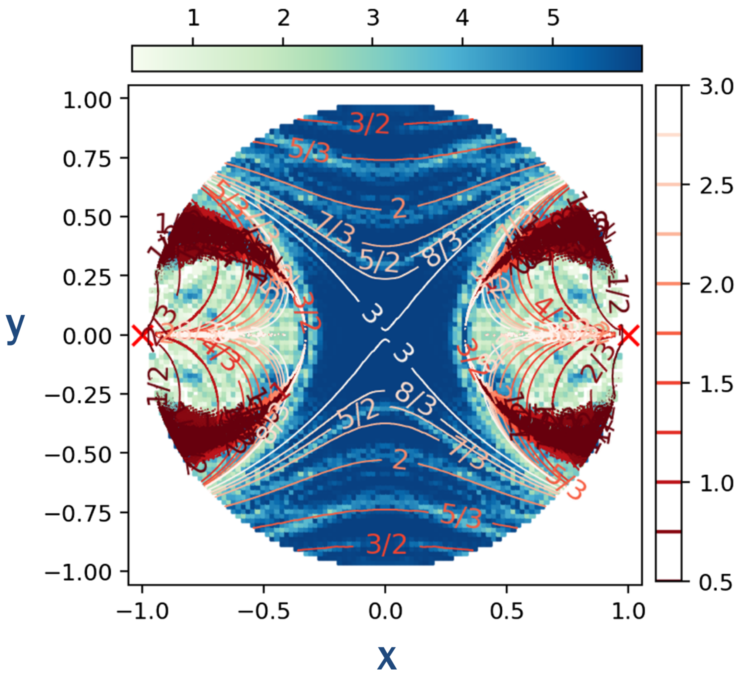

Reveals phase space regions for IOTA that are sensitive to chaos and to be avoided.

Frequency Map Analysis

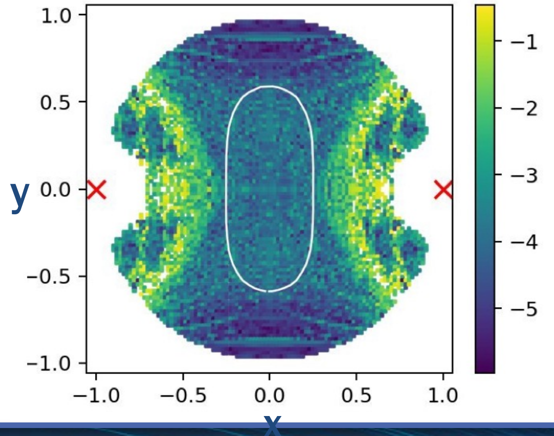

Forward-Backward Integration

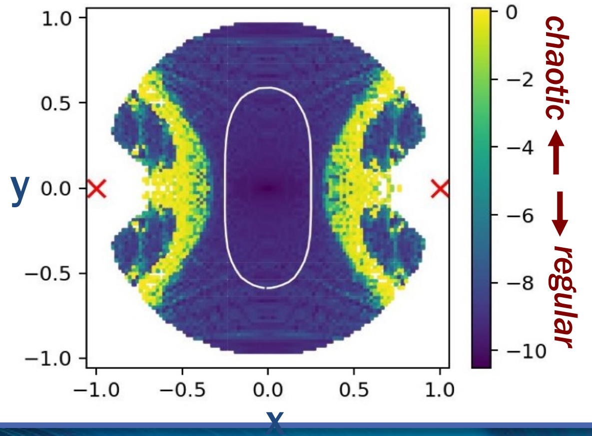

Stable aperture for halo particles surrounding a proton beam in IOTA

K. Hwang, C. Mitchell, R. Ryne, Phys. Rev. Accel. Beams 23, 0846021 (2020)

Numerical Tools in IMPACT-Z for Improved Characterization and Visualization of Proton Beam Losses in IOTA

Characterization and Visualization of Proton Losses in IOTA

- **Need:** To characterize problematic locations for losses to aid in design of diagnostics for early-stage proton operation, and to aid in selecting location/design of collimation scheme from the RFQ.
- **Problem:** Previous tracking tools available in IMPACT-Z allowed only circular/rectangular aperture, specified by element; only number of lost particles per turn was stored, without phase space information.
- **Solution:** Symplectic space charge tracking algorithm was updated to allow variable particle number; elliptical and fully s-dependent aperture capability was implemented; phase space information for all lost particles is now stored and visualized via Python interface.
- **Outcome:** Tools for visualizing proton losses were applied to compare methods for truncating the beam distribution in IOTA at the nominal emittance out of the RFQ, studying importance of mismatch, magnetic insert strength, and distribution type.

from Kilean Hwang

Physical aperture in the IOTA ring

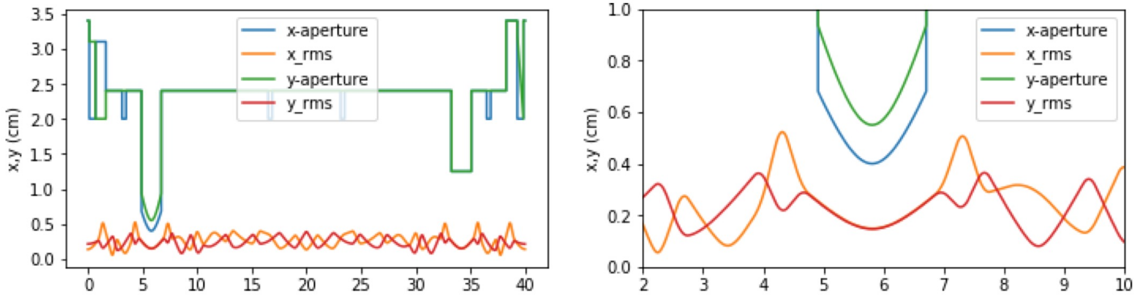

Figure: Aperture and RMS beam size. RMS beam size represent bare lattice optics with the nominal geometric emittance $\varepsilon_{x,y} = 3.3\mu m$

Visualization of beam loss for an uncollimated beam with mismatch

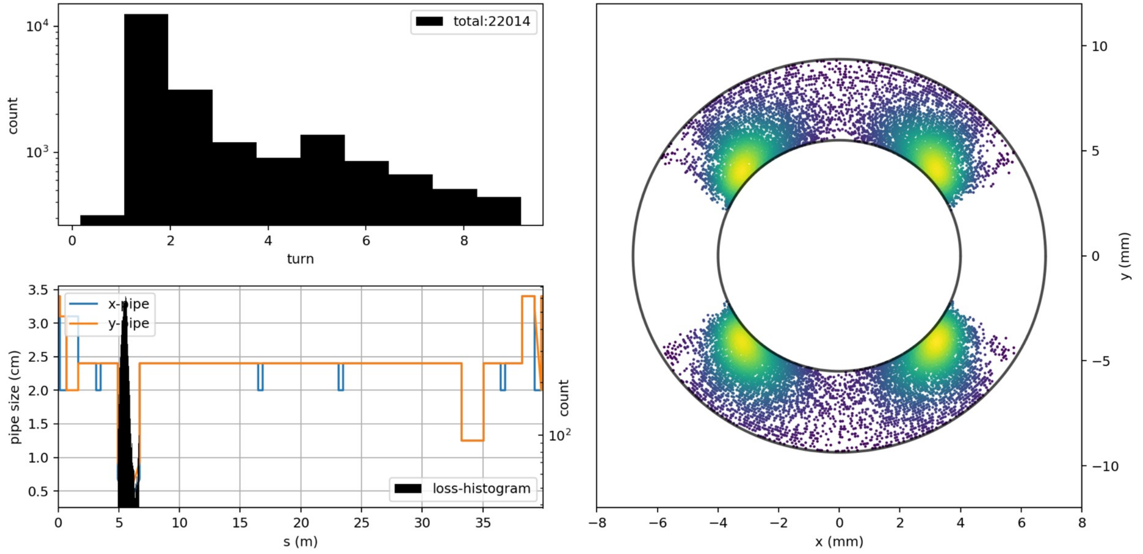

Numerical diagnostics using statistical distance (distribution "proximity") implemented to characterize a beam's relaxation to a stationary state

- **Need:** To numerically characterize "proximity" and relaxation processes for beams in the presence of high intensity or strong nonlinear focusing.

- **Problem:** Diagnostics using low-order (eg, 2nd) beam moments are insufficient to characterize "proximity" of distributions in the presence of strong nonlinear effects.

- **Solution:** Implement two-sample measures of statistical distance such as **Maximum Mean Discrepancy,** effectively embedding each distribution into a linear Hilbert space.

$$k : \mathcal{X} \times \mathcal{X} \rightarrow \mathbb{R}: \text{ symmetric positive-definite characteristic kernel}$$

$$\gamma_k(\mathbb{P},\mathbb{Q}) = \left(\int\int k(X,X')d\Delta(X)d\Delta(X')\right)^{1/2}, \quad \Delta = \mathbb{P}-\mathbb{Q}$$

C. Mitchell et al, Phys. Rev. E 106, 065302 (2022)

Distance to equilibrium as characterized by Maximum Mean Discrepancy

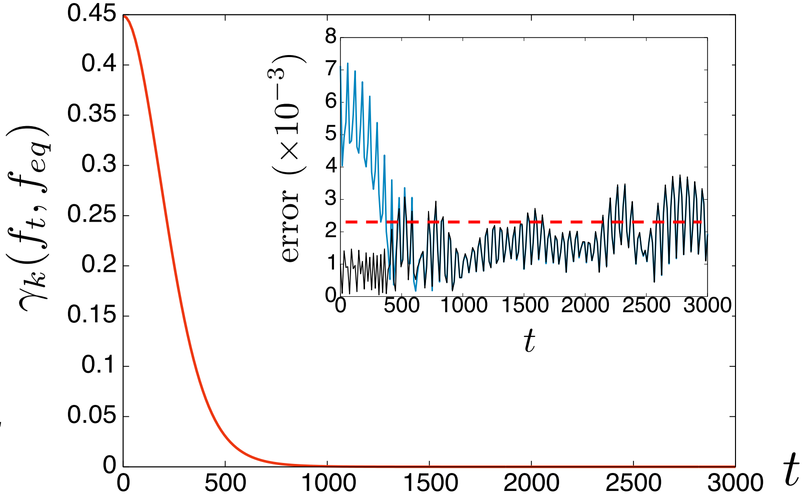

Filamentation of a beam kicked off-axis in a nonlinear focusing system

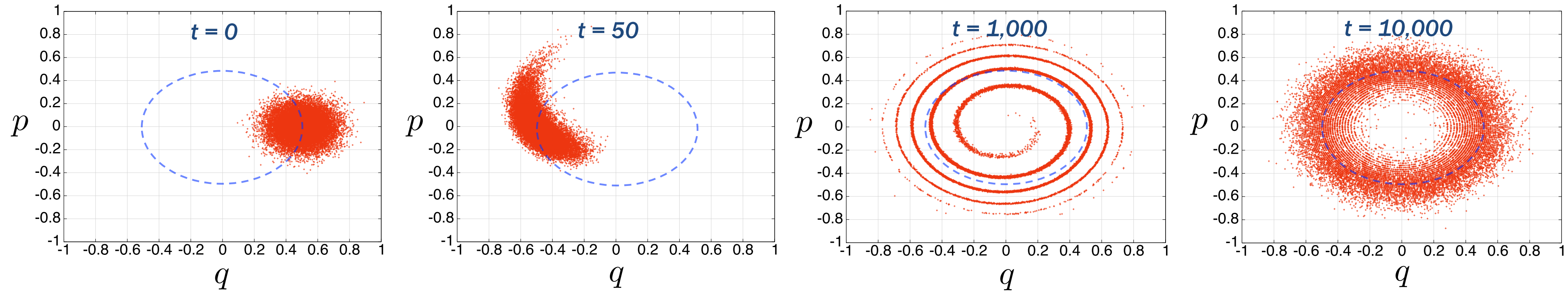

Computed with complexity O(n) for translation-invariant kernels (e.g., Gaussian)

n = number of simulated particles

Provides a quantitative metric for numerical studies of relaxation.

- Optimization for halo suppression

High-resolution modeling studies proton beam filamentation, halo, and losses in the IOTA ring and how these can be mitigated.

Impact of magnetic c-parameter on halo

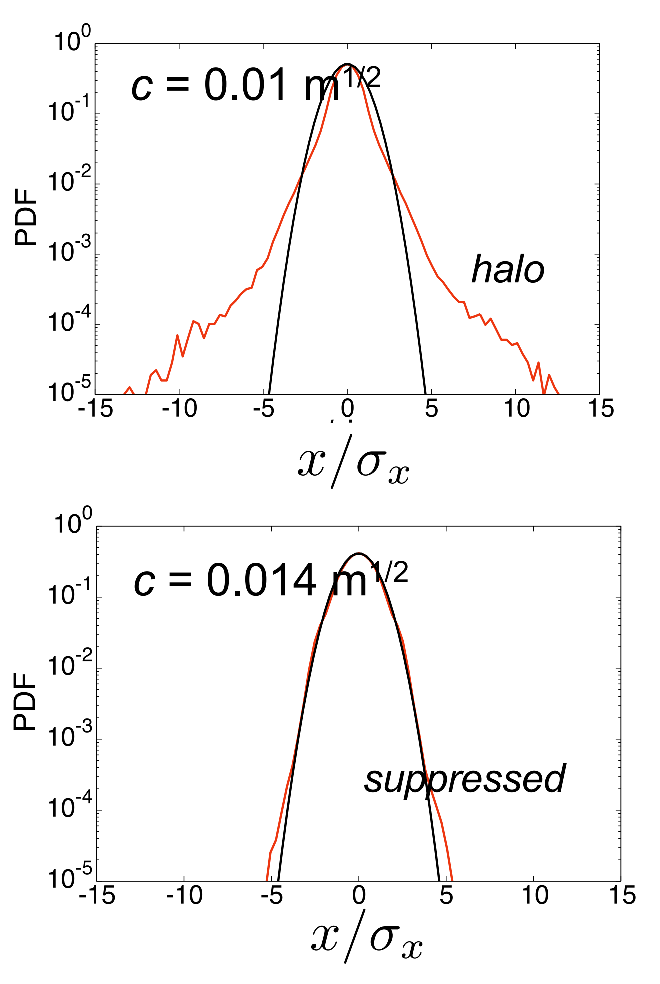

- Halo formation occurs on a time scale of 200-300 turns (at 5-8 mA).
- Due to chaos induced when particles cross a separatrix-like structure in the phase space.
- Increasing *c*-parameter of the nonlinear magnet moves the problematic separatrix farther from the beam.

Design with increased c-parameter is being explored with the vendor.

Shows existing integrable optics designs can be improved!

Intense 8 mA proton beam in IOTA (vertical phase space)

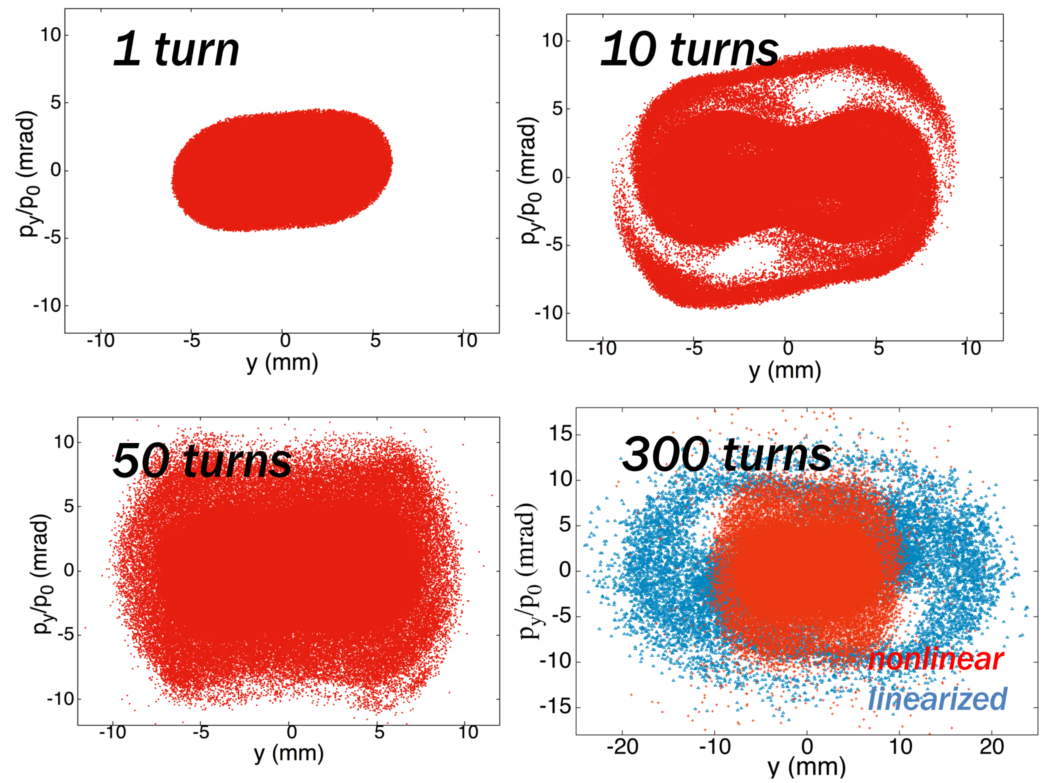

IOTA shows less halo formation than a linear design in this regime, ***but*** *results are sensitive to parameters and to the choice of linear design (mixed).*

Conclusions

- Accelerator designs based on nonlinear integrable optics have the potential to provide strong damping of instabilities (decoherence), but require a new toolkit of techniques for analysis and modeling.
- Analytical and semi-analytical methods for dynamical systems play an important role.
- For the case of the IOTA storage ring, theory and modeling reveal an unexpectedly rich single-particle dynamics, with several distinct operating regimes. Modeling reveals a mixture of regular and chaotic orbits at high intensity. Beam halo mechanisms need to be better understood, and room remains for optimization.
- Studies motivated the implementation of new tools in IMPACT-Z, including improved tracking and fringe field models (e.g., for dipoles), nonlinear magnet element types, new space charge models, new beam diagnostics, and a workflow for optimization and postprocessing using Jupyter.
- Exploring the space of possible integrable focusing lattice schemes could have a major impact on beam performance in future high intensity machines.

- **Backup material**

Integrability holds for (single-particle) motion of on-energy particles in the transverse degrees of freedom

- **Dynamics inside the nonlinear magnetic insert:**

$$H_\perp = \frac{1}{2}(P_x^2 + P_y^2) - \frac{\tau c^2}{\beta(s)} U\left(\frac{X}{c\sqrt{\beta(s)}}, \frac{Y}{c\sqrt{\beta(s)}}\right) \rightarrow H_N = \frac{1}{2}(P_{xN}^2 + P_{yN}^2 + X_N^2 + Y_N^2) - \tau U(X_N, Y_N)$$

first invariant

Courant-Snyder transformation, scaling

D&N give in [1] a realizable potential *U* such that H_N admits a second invariant I_N :

$$\{H_N, I_N\} = 0 \; .$$

- **Dynamics in the arc external to the nonlinear magnetic insert:**

Assumed *linear* with a map R_N given by:

$$R_N = \pm I \quad \text{(4x4 identity)}$$

Thus, the phase advance must be *nπ*.

H_N, I_N are invariant under the one-turn map.

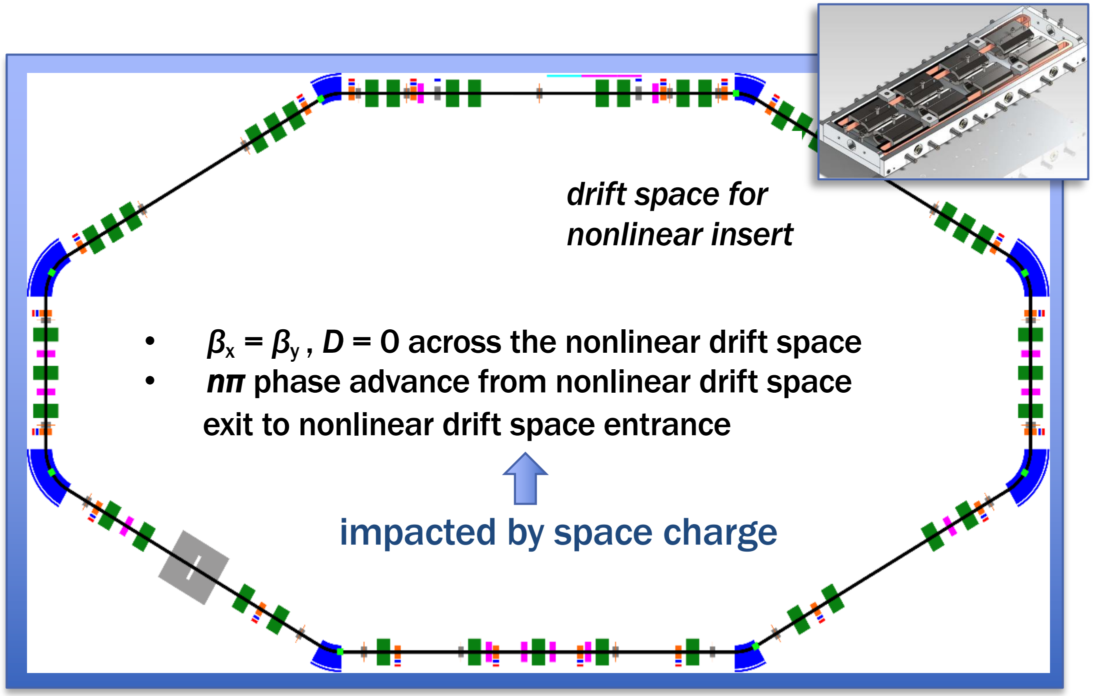

[1] V. Danilov and S. Nagaitsev, Phys Rev Accel Beams **13**, 084002 (2010)

Magnetic Vector Potential and Magnetic Field within the IOTA Nonlinear Magnetic Insert

The ideal 2D magnetic field within the nonlinear insert at location *s* is given by $\vec{B} = \nabla \times \vec{A} = -\nabla\psi$, where the potentials are given in terms of dimensionless quantities:

$$F = \frac{A_s + i\psi}{B\rho}, \quad z = \frac{x+iy}{c\sqrt{\beta(s)}}, \quad \tilde{t} = \frac{\tau c^2}{\beta(s)}$$

using the complex function:

$$F(z) = \left(\frac{\tilde{t}z}{\sqrt{1-z^2}}\right) \arcsin(z) \; .$$

The transverse focusing fields vary longitudinally with *s*.

$$\frac{\beta(s)}{\beta*} = 1 + \left(\frac{2s}{L}\right)^2 \tan^2 \pi\mu_0, \qquad \beta^* = \frac{L}{2}\cot\pi\mu_0, \quad 0 < \mu_0 < 1/2$$

L – length of the magnetic insert [m]
$2\pi\mu_0$ – phase advance across the magnetic insert
β^* - beta function at the longitudinal midpoint

Magnetic field lines in the transverse plane

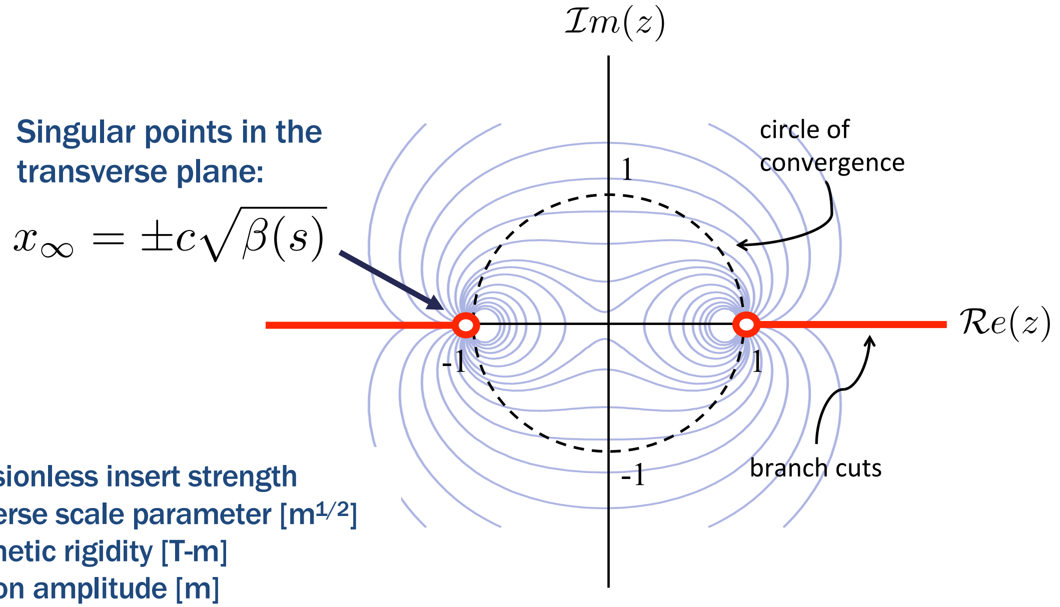

τ – dimensionless insert strength
c – transverse scale parameter [$m^{1/2}$]
Bρ – magnetic rigidity [T-m]
β – betatron amplitude [m]

Longitudinal variation of the quadrupole gradient

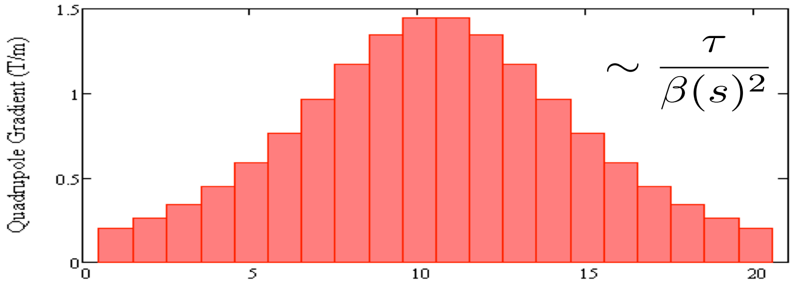

Critical and resonance structures in the single-particle phase space (zero current integrable motion)

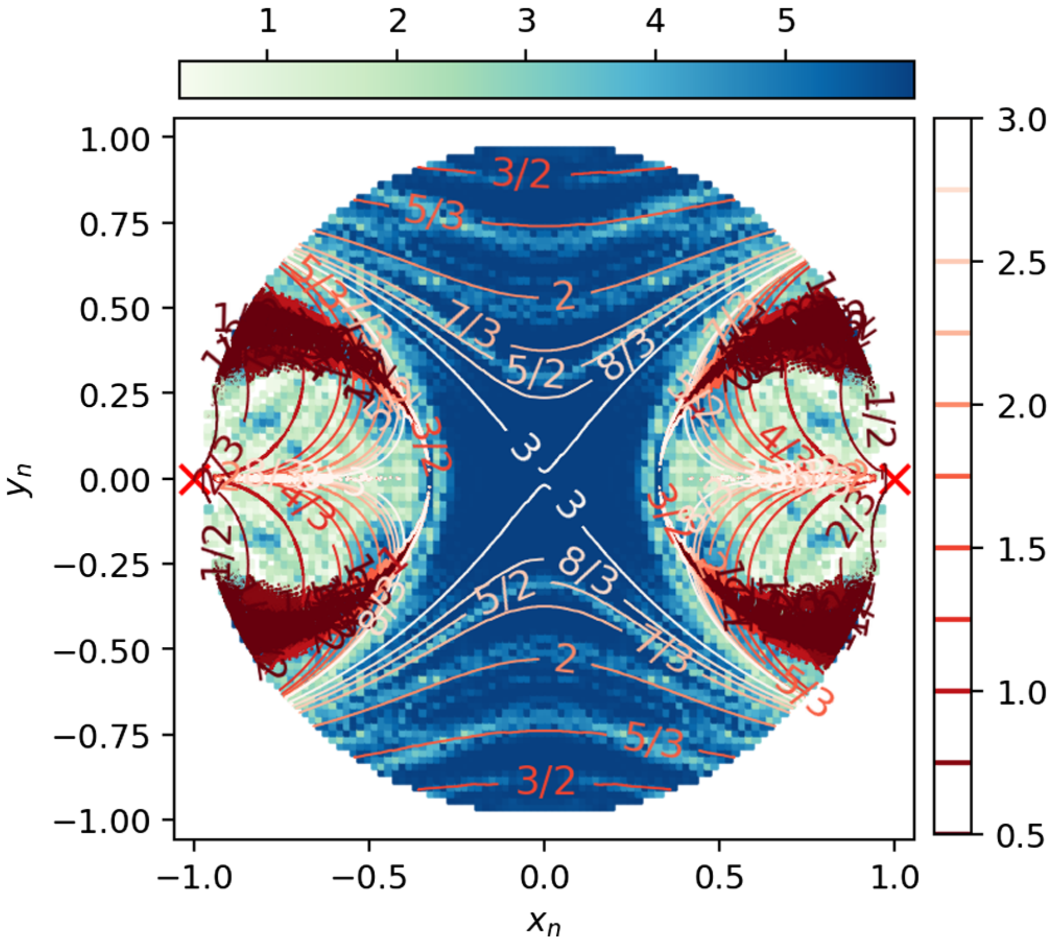

Critical structures:

- Red curve: primary separatrix-like structure
  Black curve: I.C.s for unstable periodic orbits
- Separate regions of distinct orbit behavior
- A matched beam at 0 mA with the nominal emittance lies within the primary separatrix

Resonance structures:

- Resonant contour lines ν_y/ν_x are shown
- High density of resonances outside the primary separatrix
- Color: measure of chaos when phase advance is perturbed (blue = regular)

When the phase advance is depressed, chaos develops first in the region outside the primary separatrix.

K. Hwang *et al*, Phys. Rev. Accel. Beams 23, 084602 (2020)
C. Mitchell *et al*, Phys. Rev. Accel. Beams 23, 064002 (2020)

Critical and resonance structures in the single-particle phase space (zero current integrable motion)

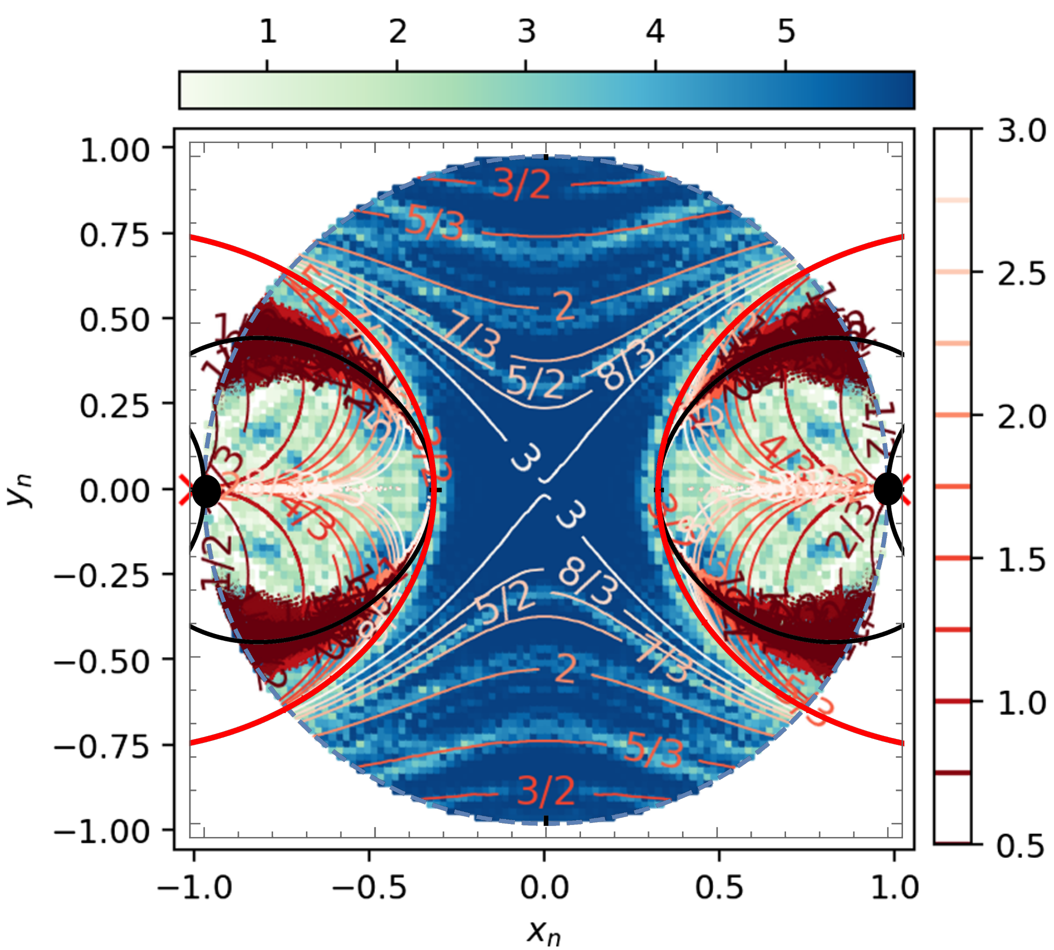

Critical structures:

- Red curve: primary separatrix-like structure
  Black curve: I.C.s for unstable periodic orbits
- Separate regions of distinct orbit behavior
- A matched beam at 0 mA with the nominal emittance lies within the primary separatrix

Resonance structures:

- Resonant contour lines ν_y/ν_x are shown
- High density of resonances outside the primary separatrix
- Color: measure of chaos when phase advance is perturbed (blue = regular)

When the phase advance is depressed, chaos develops first in the region outside the primary separatrix.

K. Hwang *et al*, Phys. Rev. Accel. Beams 23, 084602 (2020)
C. Mitchell *et al*, Phys. Rev. Accel. Beams 23, 064002 (2020)

Surface Methods Provide a Robust Method for Tracking in the IOTA Nonlinear Magnetic Insert with Realistic 3D Fringe Fields

- **Need:** Accurate symplectic tracking algorithm for modeling the IOTA nonlinear magnetic insert with realistic fringe fields.

- **Problem:** The standard idealized model of the IOTA insert is non-Maxwellian, and neglects fringe field effects. 3D magnetic field data inherently noisy.

- **Solution:** Use surface methods to extract a smooth vector potential from 3D magnetic field data.

- **Outcome:** Tracking with quadrupole and octupole fringe field corrections shows evidence of perturbed invariants, with little evidence of enhanced losses (10K turns).

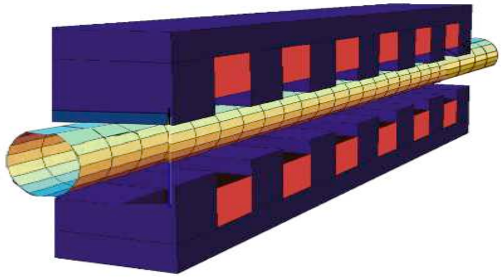

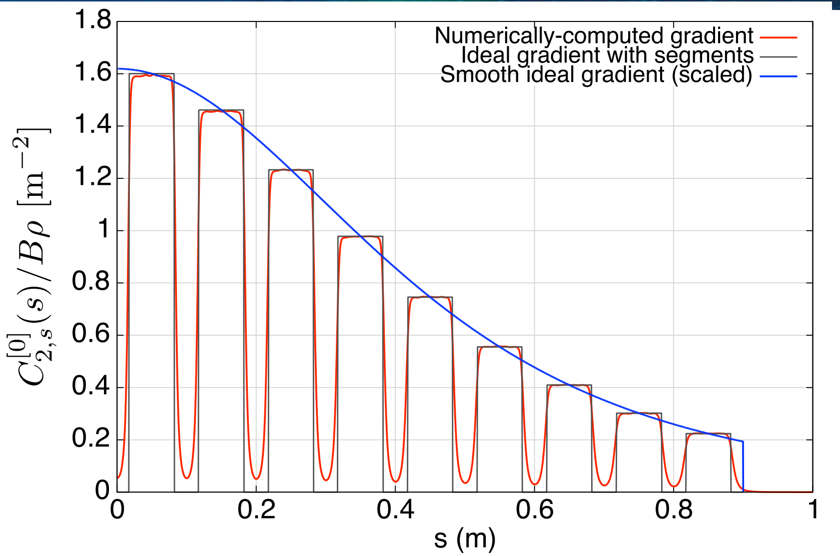

$$C_{m,\alpha}^{[n]}(s) = \frac{i^n}{2^m m!}\int_{-\infty}^{\infty}\frac{k^{n+m-1}}{I'_m(kR)}\tilde{B}_\rho^\alpha(R,m,k)e^{iks}dk$$

$$H = -\sqrt{1-\frac{2P_t}{\beta_0}+P_t^2-(\vec{P}-\vec{\mathcal{A}}_\perp)^2}-\mathcal{A}_s-\frac{1}{\beta_0}P_t$$

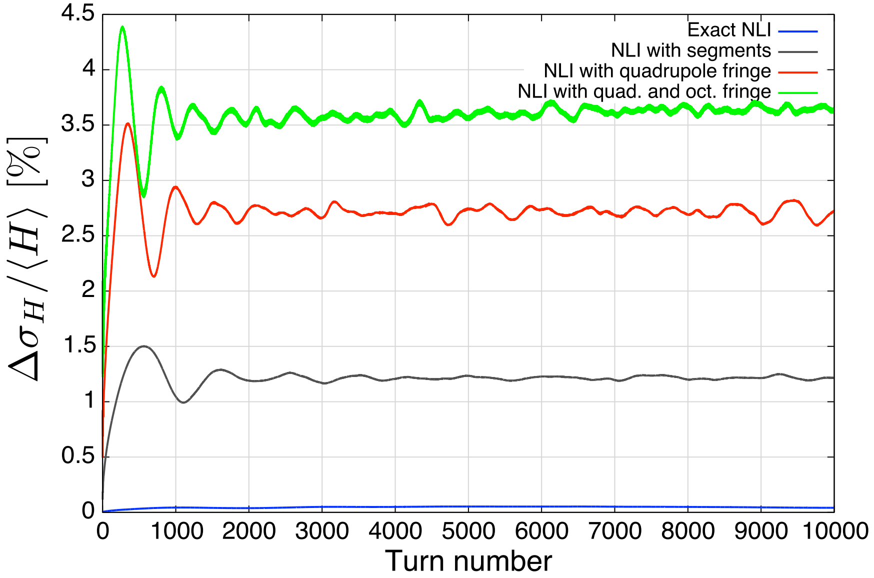

C. Mitchell, Proc IPAC2018, Vancouver, THPAK036 (2018).

Effect of the Increasing the c Value on the Matched Beam Distribution in Invariant Space

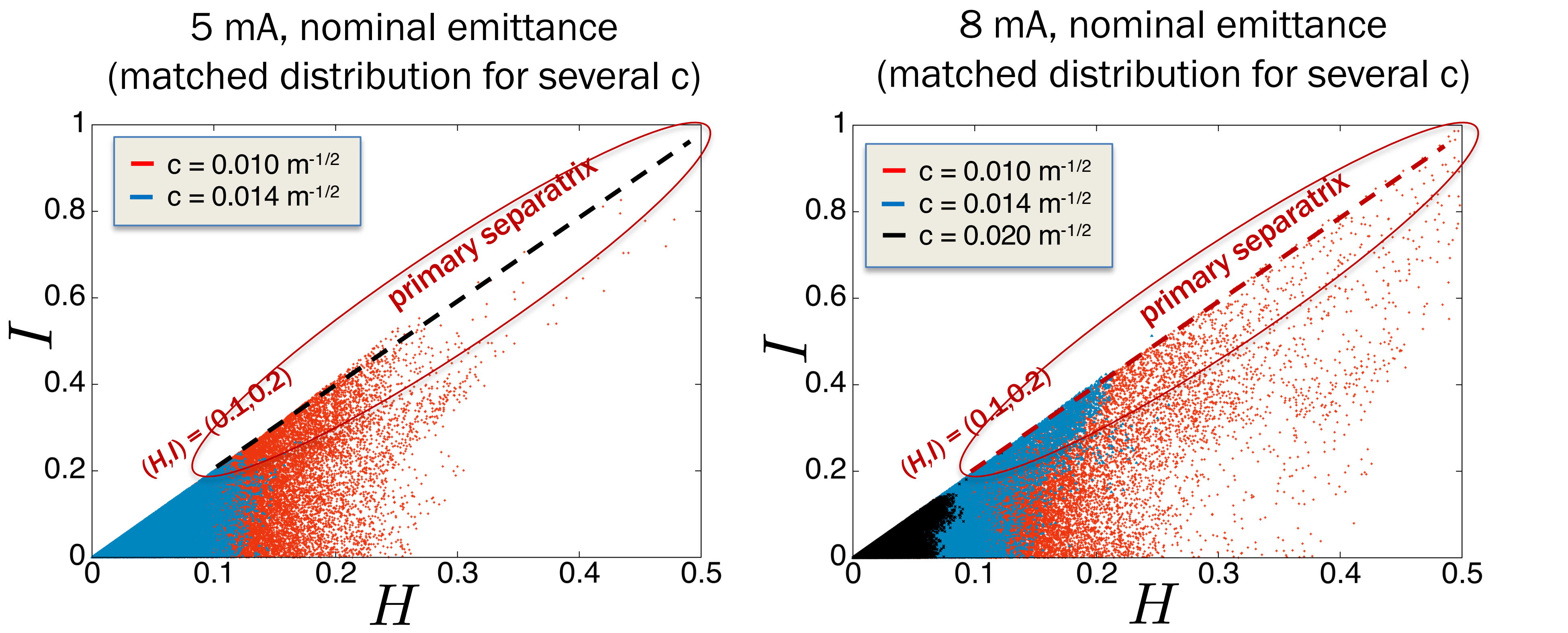

- Increasing the c value leads the beam footprint to shrink in invariant space.
- The primary separatrix begins at (H,I)=(0.1,0.2) and extends along the ray I = 2H
- For sufficiently large c, the beam can be confined away from the primary separatrix.

Understanding Proton Beam Dynamics at High Space Charge Intensity: An Example of Code Benchmarking (IMPACT-Z & MaryLie/IMPACT)

Goal: Study relaxation of a beam in IOTA to near-equilibrium at high intensity, to compare with halo formation in a standard linear lattice.

- Physical IOTA lattice, 2.5 MeV proton beam with nominal emittance and energy spread.
- 8 mA beam current ($\Delta Q_y \approx$-0.6, $\Delta Q_x \approx$-0.9) – near maximum for expected IOTA operation.

Comparing beam size over turn 10

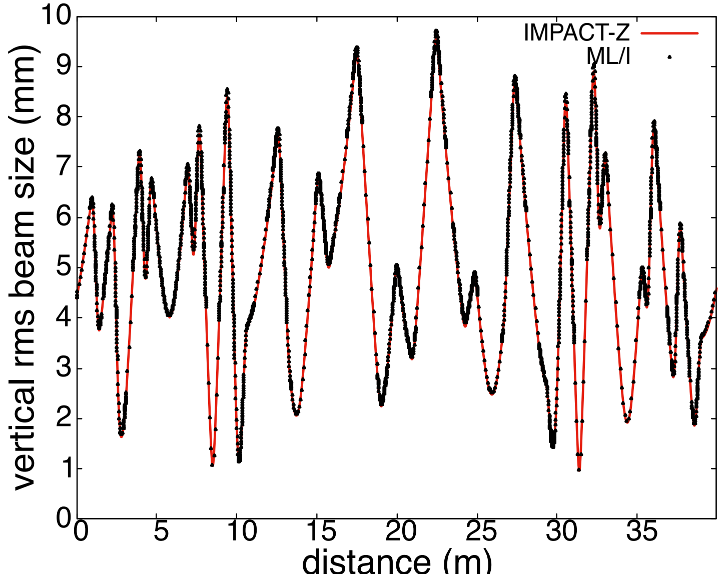

Comparing beam after 10 turns

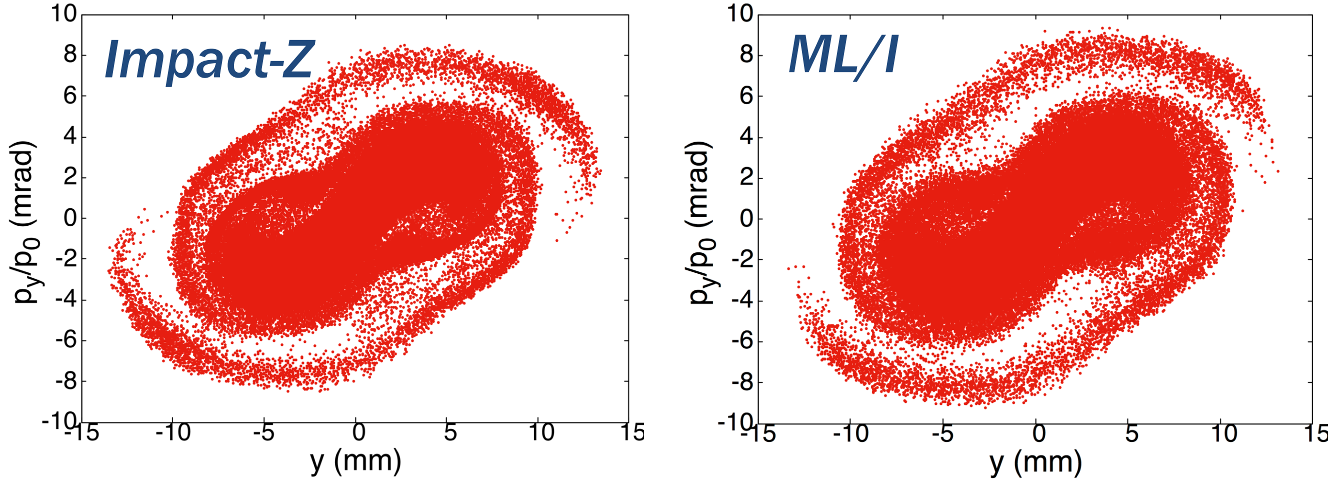

Reasonable agreement between two codes using different space charge algorithms (spectral, PIC).

Numerical convergence tests: # modes/grid points, # particles, location of Poisson boundary, # sc kicks.

Frequency map analysis of orbits in the total potential (space charge + focusing) for a stationary beam in a nonlinear constant focusing channel.

- Extreme current (space charge tune shift >1 near the origin), shown for illustration purposes only.
- 8K distinct initial conditions (*x,0,y,0*) in a disk.
- Orbits are tracked in the sum of the external potential and the equilibrium space charge potential (using 15x15 modes) for 2048 x 1.8 m distance through the nonlinear constant focusing section.

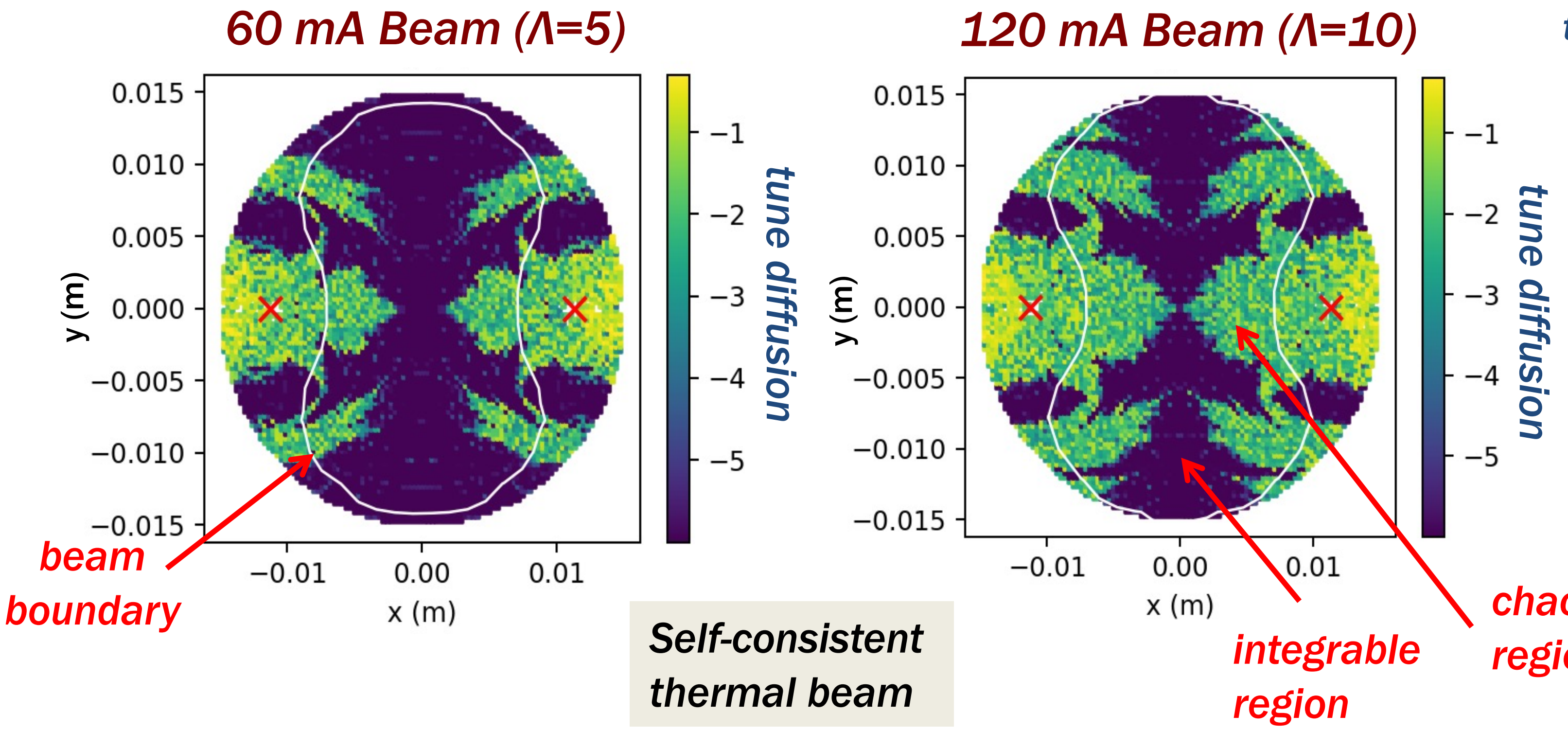

Singular points of the NL potential at:

$$(\pm 1.13\ \mathrm{cm}, 0)$$

Motion is bounded due to H conservation.

Integrable region shrinks with increasing current.